To the Graduate Council:

I am submitting herewith a thesis written by Woo-kum Lee entitled "Thermal Radiation Heat Transfer of Non-Newtonian Fluid along a Needle." I have examined the final copy of this thesis for form and content and recommend that it be accepted in partial fulfillment of the requirements for the degree of Master of Science, with a major in Engineering Science.

K.H. Kim, Major Professor

We have read this thesis and
recommend its acceptance:

Osama Soliman

Carl J. Remenyik

Accepted for the Council:

Vice Provost
and Dean of The Graduate School

STATEMENT OF PERMISSION TO USE

In presenting this thesis in partial fulfillment of the requirements for a Master's degree at The University of Tennessee, Knoxville, I agree that the Library shall make it available to borrowers under rules of the Library. Brief quotations from this thesis are allowable without special permission, provided that accurate acknowledgement of the source is made.

Permission for extensive quotation from or reproduction of this thesis may be granted by my major professor, or in his absence, by the Head of Interlibrary Services when, in the opinion of either, the proposed use of the material is for scholarly purposes. Any copying of use of the material in this thesis for financial gain shall not be allowed without my written permission.

Signature Woo-kum Lee.

Date December 2. 1988

THERMAL RADIATION HEAT TRANSFER OF NON-NEWTONIAN FLUID ALONG A NEEDLE

A Thesis

Presented for the

Master of Science

Degree

The University of Tennessee, Knoxville

Woo-kum Lee

December 1988

DEDICATION

This work is dedicated to my parents.

ACKNOWLEDGEMENTS

My deepest appreciation and thanks go to Dr. K.H.Kim, who acted as my advisor. He provided many helpful suggestions and direction whenever I encountered with difficulties during the course of this research. Special gratitudes also extended to Dr. C.J. Remenyik and Dr. M.O. Soliman who served as members of my thesis committee.

ABSTRACT

The purpose of this study was to investigate laminar natural convection heat transfer along a thin needle in non-Newtonian fluids. Particular interest was to examine the heat transfer rate and the skin friction as well as the similarity velocity and temperature profiles for different non-Newtonian fluid indices, n. Also this study examined the behavior of non-Newtonian power-law fluid due to the effects of thermal radiation heat transfer and different needle sizes as well as various Prandtle numbers. The study was initiated by determining a set of transformation variables which reduced the original boundary layer equations to the ordinary differential equations.

The technique of numerical analysis used to obtain these ordinary differential equations was the Runge-Kutta algorithm. This algorithm was used to generate solutions based on corrections to initial guesses for the initial values given to the slopes of the velocity profiles and temperature profiles at the wall. The corrections were obtained by satisfying the asymptotic boundary layer so that the mean square errors between the computed variables and the asymptotic values are minimized.

Solutions of these equations were based on incompressible, viscous flow where the properties such as viscosity and thermal conductivity were assumed to be constant. The radiation properties of the medium were assumed to be optically thick. For an optically thick medium, a diffusion approximation or Rosseland approximation can be applied. In the optically thick medium, the radiation heat flux can not travel a long distance because the medium is optically dense. Therefore, the radiation heat transfer may be considered as heat conduction. The radiation heat flux term was simplified by means of Rosseland approximation. Then this term was linearized by using the Taylor expansion. The momentum and temperature profiles were presented for various Prandtl numbers and

conduction to radiation parameter as well as several non-Newtonian cases according to different values of n. The results show the effects of radiation, Prandtl numbers and needle shape on non-Newtonian fluid as well as the Newtonian fluid.

TABLE OF CONTENTS

CHAPTER	PAGE
I. INTRODUCTION	1
II. THEORETICAL ANALYSIS OF THE NON-NEWTONIAN POWER-LAW FLUID	4
Considerations of the non-Newtonian Fluids	4
Formulation of Fundamental Equations	5
Similarity Transformation	14
III. ANALYSIS OF THE SIMILARITY SOLUTION	22
Satisfaction of the Asymptotic Boundary Conditions	22
Results of the Solution Algorithm	28
IV. CONCLUSIONS AND RECOMMENDATIONS	52
LIST OF REFERENCES	54
APPENDIX	57
VITA	70

LIST OF TABLES

TABLE **PAGE**

1. The value of the needle shape partameter η_∞, dx, and the maximum error according to different Prandtl numbers 29

LIST OF FIGURES

FIGURE		PAGE
1.	Needle geometry of the problem	6
2.	Similarity velocity profile with $\eta_o = 0.1$ and no radiation in non-Newtonian fluid (n = 1.2)	32
3.	Similarity temperature profile with $\eta_o = 0.1$ and no radiation in non-Newtonian fluid (n = 1.2)	33
4.	Similarity velocity profile with $\eta_o = 0.1$ and no radiation in Newtonian fluid (n = 1.0)	34
5.	Similarity temperature profile with $\eta_o = 0.1$ and no radiation in Newtonian fluid (n = 1.0)	35
6.	Similarity velocity profile with $\eta_o = 0.1$ and no radiation in non-Newtonian fluid (n = 0.8)	36
7.	Similarity temperature profile with $\eta_o = 0.1$ and no radiation in non-Newtonian fluid (n = 0.8)	37
8.	Similarity velocity profile with $\eta_o = 0.1$ and Pr = 100 in non-Newtonian fluid (n = 1.2)	38
9.	Similarity temperature profile with $\eta_o = 0.1$ and Pr = 100 in non-Newtonian fluid (n = 1.2)	39
10.	Similarity velocity profile with $\eta_o = 0.1$ and Pr = 100 in Newtonian fluid (n = 1.0)	40
11.	Similarity temperature profile with $\eta_o = 0.1$ and Pr = 100 in Newtonian fluid (n = 1.0)	41
12.	Similarity velocity profile with $\eta_o = 0.1$ and Pr = 100 in non-Newtonian fluid (n = 0.8)	42
13.	Similarity temperature profile with $\eta_o = 0.1$ and Pr = 100 in non-Newtonian fluid (n = 0.8)	43

14. Similarity velocity profile with $\eta_o = 0.1$, Pr = 100 and radiation effect (N = 1.0) 44
15. Similarity temperature profile with $\eta_o = 0.1$, Pr = 100 and radiation effect (N = 1.0) 45
16. Similarity velocity profile with $\eta_o = 0.001$, Pr = 100 and radiation effect (N = 1.0) 46
17. Similarity temperature profile with $\eta_o = 0.001$, Pr = 100 and radiation effect (N = 1.0) 47
18. Similarity velocity profile with $\eta_o = 0.1$, Pr = 100 and no radiation (N = infinity) 48
19. Similarity temperature profile with $\eta_o = 0.1$, Pr = 100 and no radiation (N = infinity) 49
20. Similarity velocity profile with $\eta_o = 0.001$, Pr = 100 and no radiation (N = infinity) 50
21. Similarity temperature profile with $\eta_o = 0.001$, Pr = 100 and no radiation (N = infinity) 51

LIST OF SYMBOLS

A	similarity transformation parameter
α	thermal diffusivity
a_λ	absorption coefficient
β	thermal expansion coefficient
c_p	specific heat
D_λ	extinction coefficient
d_λ	optical thickness
δ_λ	scattering coefficient
E	error term
f	stream function in similarity transformation
f'	similarity velocity function
f''	transformed skin friction
g	similarity temperature function
g'	transformed heat transfer rate
G_r	generalized Grashof number $\left(= L^{(n+2)} \dfrac{\left\{g\beta\,(T_w - T_\infty)\right\}^{(2-n)}}{\nu^2} \right)$
g_z	gravitational constant
η	independent similarity variable
$\eta_\circ$	needle shape parameter
k	thermal conductivity
L	characteristic length
m	reflective index
μ	dynamic viscosity

N	conduction to radiation parameter $\left(= \frac{kD_\lambda}{4\sigma m^2 T_\infty^3} \right)$
n	non-Newtonian flow behavior index
ν	kinematic viscosity
p	pressure
p_r	generalized Prandtl number $\left(= \nu^{(2/1+n)} \; L^{(1-n/1+n)} \; \frac{\left\{ g\beta L \, (T_w - T_\infty) \right\}^{\frac{3(n-1)}{2(n+1)}}}{\alpha} \right)$
q_r	radiative heat flux
θ	dimensionless temperature
r, z	spatial variables in real dimension
r^*, z^*	spatial variables in non-dimensional form
ρ	density
s	thickness of medium
σ	Stefan-Boltzmann constant
T	temperature
T_∞	free stream temperature
τ	shear stress
$u_\circ$	characteristic velocity $\left(= \sqrt{g\beta L \, (T_w - T_\infty)} \right)$
v_r, v_z	z and r velocity in real dimension
v_r^*, v_z^*	z and r velocity in non-dimensional form
ψ	stream function

subscript

$\circ$	denotes the condition at the wall
∞	denotes the condition at the edge of the boundary layer

superscript

*	denotes the non-dimensional form

CHAPTER I

INTRODUCTION

Recent year has seen a rapid intensification of research related to the measurement, prediction, and understanding of heat transfer by natural convection. For external natural convection, the measurements and predictions have focussed on problems where the flow is two-dimensional (e.g., vertical plates and cylinders, tilted plates, horizontal circular cylinders) or axisymmetric (e.g., spheres). In particular, the increasing use of many non-Newtonian fluids in chemical process industries has necessitated the understanding of their behavior in many transport processes. The prediction of heat transfer rates and shear stress for external flows of non-Newtonian fluids, is therefore, of practical interest.

While applying the numerical and analytical tools to solve the problems of fluid dynamics and heat transfer for non-Newtonian fluids, a number of complications arises due to the non-linear relation between the stress tensor and deformation strain tensor. S.Y. Lee and W.F. Ames [1] suggested various empirical models for non-Newtonian fluids.

Several investigators reported various problems of non-Newtonian fluids. Acrivos et al. [2] have presented theoretical analysis of flow past an external surface of power-law fluids under forced convection. Schowalter [3] has shown that similar solutions exist for externals flows (of power-law non-Newtonian fluids) over a wedge by reducing three dimensional boundary layer equations to ordinary differential equations. Ames and Lee [1] have critically reviewed the existing important similar solutions available in literature, for boundary layer flows of non-Newtonian fluids. They have applied transformation group method to obtain similarity variables and equations for various types of flows. Also a few

investigators examined various needle problems. T. Cebeci and Y. Na [4] obtained the similarity solution of an isothermal vertical needle problem and T. Govindarajulu [5] solved the non-isothermal needle problem by using the similarity technique. J. P. Naran and M.S. Uberoi [6] described the laminar free convection from vertical thin needles with uniform heat flux. J.L.S. Chen [7,8] investigated the free convection from vertical needles with variable wall temperature and variable wall heat flux.

The results presented in these investigations did not include the effects of thermal radiation. Numerous papers related to the thermal radiation effects were published. In 1962, Viskanta and Gosh [9] reported the problem of laminar flow over a wedge for the optically thick boundary layer. Novotny and Yang (1967), and Goulard (1964), investigated the optically thick approximation for boundary layer flow over flat plate for a Newtonian fluid [10,11]. Kim and Ozisik published several papers in this field, especially in the area of thermal radiation effects in boundary layer flow [12,13] . Galuska and Kim [14], solved the problem of laminar natural convection heat transfer for non-Newtonan fluids in 1982.

Considerable efforts have been usefully devoted to forced convection and natural convection, as well as combined convection heat transfer in non-Newtonian fluids. However, most of these investigations were considered with flat plate in the non-Newtonian fluids. This research investigates the laminar boundary layer flow along a thin needle in power-law non-Newtonian fluids; effects of the non-Newtonian fluid behavior and the needle size on the flow are examined and radiation effects are investigated.

In the present investigation, the momentum and energy equations will be developed in the boundary layer along a vertical thin needle. Also the Rosseland approximation is employed to represent heat flux due to thermal radiation. In chapter II, brief explanations of the non-Newtonian power-law fluid and the thermal radiation with the Rosseland

approximation will be presented. And then the derivation of similarity equations will be shown. In chapter III, the analysis of the similarity solution and results are discussed in detail. Similarity velocity profiles and temperature profiles are obtained. Results are presented for flow behavior indices (n) of 0.8 and n=1.2, as well as for the Newtonian case n=1.0. Finally, the conclusions and recommendations will be given in chapter IV. The computer codes used in the analysis are listed in the appendix.

CHAPTER II

THEORETICAL ANALYSIS OF THE NON-NEWTONIAN POWER-LAW FLUID

2.1 Considerations of non-Newtonian fluids

The linear relationship between stress and strain rate is considered in the classical theory of fluid mechanics; the shear stress imposed on the fluid is directly proportional to the rate of strain. This linear relationship for one-dimensional or boundary layer types of flow is defined by

$$\tau = -\mu\frac{\partial v}{\partial y} \tag{2-1}$$

Fluids with properties different from the equation (2-1) are called non-Newtonian fluids. The term "non-Newtonian fluids" is one of very great generality and includes all fluids for which the equations of classical hydrodynamics do not apply. The non-Newtonian fluids are generally divided into two categories. One is the viscoelastic fluids, where the stress depends on both the instantaneous strain rate and the past strain history. The other is the viscoinelastic fluids, where the stress depends on the current state of strain only.

There are three kinds of empirical equations for the non-Newtonian fluids.

1. Bingham plastics:

$$\tau = - k_1 \frac{\partial v}{\partial y} \pm \tau_\circ \qquad \text{if } |\tau| > \tau_\circ$$

$$\frac{\partial v}{\partial y} = 0 \qquad \text{if } |\tau| < \tau_\circ$$

where

k_1 is empirical constant and $\tau_\circ$ is the yield stress.

2. Eyring viscous fluids:

$$\tau = - k_4 \left\{ 1 - \frac{\sinh^{-1}\left(k_2 \frac{\partial v}{\partial y}\right)}{k_3 \frac{\partial v}{\partial y}} \right\}$$

where

k_2, k_3 and k_4 are empirical constants.

3. Power-law fluids:

$$\tau = - k\left(\frac{\partial v}{\partial y}\right)^n$$

where

k and n are empirical constants.

In this study the power-law fluids are considered. These power-law type fluids are characterized with satisfactory accuracy for boundary layer flow. These non-Newtonian power-law fluids also include the Newtonian fluids as a special case (n = 1). The needle geometry of the problem is shown in Fig.1.

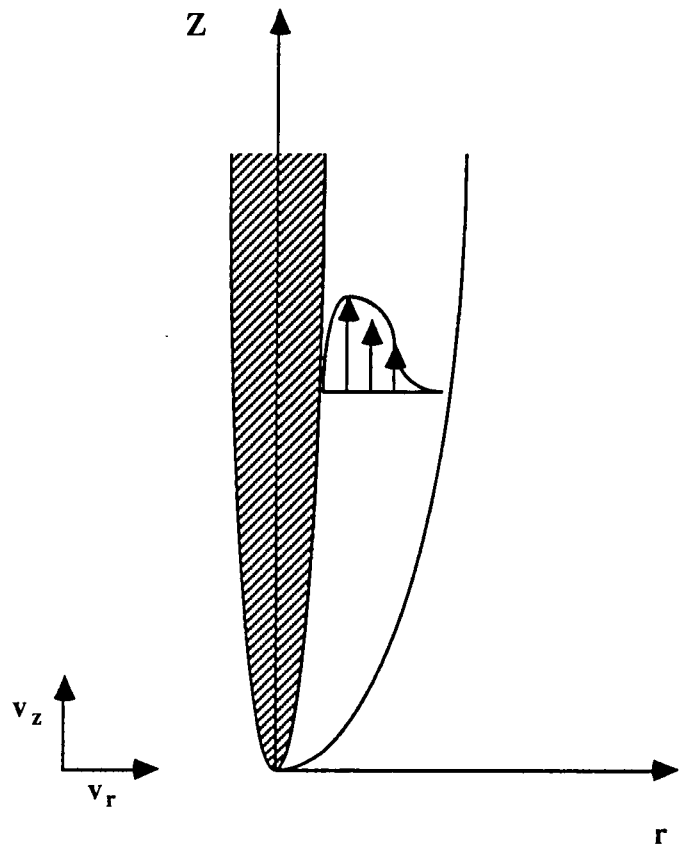

Fig.1. Needle geometry of the problem

2.2 Formulation of fundamental equations

In natural convection the movement of fluid is due to the variation of densities which is caused by the temperature difference. The momentum and energy equations are considered in this field.

This research focuses on the velocity and temperature variations along the needle in non-Newtonian fluids when the needle shape and value of parameters of conduction to radiation ratio vary. In this study, the following assumption will be employed.

1. Flow is laminar.
2. Most fluid properties remain constant.
3. Dissipation may be ignored.
4. Radiation properties of the medium are not dependent on the frequencies.
5. Radiation transport through the medium affects only molecules in close proximity.

The functional relation between the stress and the state of motion of the non-Newtonian power-law fluid is defined by

$$\tau = - \mu \left(\frac{\partial v_z}{\partial r} \right)^n \qquad (2\text{-}2)$$

with $n < 1.0$ for pseudoplastics and $n > 1.0$ for dilatant substances. When the constant n is equal to 1, this is the Newtonian fluid.

The boundary layer equations of continuity and momentum expressed using the non-Newtonian stress tensor (2-2) are

$$\frac{\partial v_r}{\partial r} + \frac{1}{r} v_r + \frac{\partial v_z}{\partial z} = 0 \tag{2-3}$$

and

$$\rho \left(v_r \frac{\partial v_z}{\partial r} + v_z \frac{\partial v_z}{\partial z} \right) = - \frac{\partial p}{\partial z} + \frac{\mu}{r} \frac{\partial}{\partial r} \left\{ r \left(\frac{\partial v_z}{\partial r} \right)^n \right\} - \rho g_z \tag{2-4}$$

There is also a concern about the temperature distribution in the boundary layer. The energy equation is expressed as

$$\rho c_p \left(v_r \frac{\partial T}{\partial r} + v_z \frac{\partial T}{\partial z} \right) = k \left(\frac{1}{r} \frac{\partial T}{\partial r} + \frac{\partial^2 T}{\partial r^2} \right) - \frac{\partial q_r}{\partial r} - \frac{1}{r} q_r \tag{2-5}$$

where

q_r = thermal radiative heat flux

k = thermal conductivity of the fluid.

The momentum equation may be derived in a more convenient form by first noting that no body force acts in the r direction. Hence the z-pressure gradient at any point in the boundary layer must equal the pressure gradient in the quiescent region outside the boundary layer.

$$\frac{\partial p}{\partial z} = - \rho_\infty g_z \tag{2-6}$$

Substituting equation (2-6) into (2-4), the momentum equation becomes

$$\rho \left(v_r \frac{\partial v_z}{\partial r} + v_z \frac{\partial v_z}{\partial z} \right) = \frac{\mu}{r} \frac{\partial}{\partial r} \left\{ r \left(\frac{\partial v_z}{\partial r} \right)^n \right\} - \left(\rho - \rho_\infty \right) g_z \tag{2-7}$$

By Taylor series ρ can be obtained as

$$\left(\rho - \rho_{\infty}\right) = -\rho\beta\left(T - T_{\infty}\right) \tag{2-8}$$

where

β = thermal expansion coefficient.

Substituting equation (2-8) into (2-7), the momentum equation (2-7) is simplified as

$$\left(v_r\frac{\partial v_z}{\partial r} + v_z\frac{\partial v_z}{\partial z}\right) = \frac{\nu}{r}\frac{\partial}{\partial r}\left\{r\left(\frac{\partial v_z}{\partial r}\right)^n\right\} + \left(T - T_{\infty}\right)\beta g_z \tag{2-9}$$

where

ν = kinematic viscosity.

The energy equation will be derived with the radiative heat flux term. As the radiation passes through the layer, its intensity is reduced by absorption and scattering. The change in intensity has been found experimentally to depend on the magnitude of the local intensity. At this point, a coefficient of D_λ which depends on the local properties of medium is introduced. The D_λ is the extinction coefficient of the material in the layer. The extinction coefficient D_λ is composed of two parts, an absorption coefficient a_λ and a scattering coefficient δ_λ.

$$D_\lambda = a_\lambda + \delta_\lambda \tag{2-10}$$

The relation between optical thickness d_λ and extinction coefficient D_λ is written by

$$d_\lambda(s) = \int_0^s D_\lambda(s)ds \tag{2-11}$$

where

s = thickness of medium.

The optical thickness or opacity is a measure of the ability of a given path length of gas to attenuate radiation of a given wave length. Therefore, a large optical thickness means large attenuation.

If the extinction coefficient D_λ is independent of temperature and pressure, the optical thickness of the medium becomes

$$d_\lambda = D_\lambda s \tag{2-12}$$

The optical thickness d_λ depends on the extinction coefficient and the thickness of the layer. When $d_\lambda >> 1$, the medium is optically thick. When $d_\lambda << 1$, the medium is optically thin.

In this study, the case which is optically thick is examined. For an optically thick medium a diffusion approximation or Rosseland approximation can be applied. In this approximation, since the medium is optically dense, the radiation can travel only a short distance before being absorbed. Hence the conditions at a local position in the medium are only influenced by closely surrounding conditions and the radiative transport becomes somewhat like heat conduction. This approximation is written as

$$q_r = -\frac{4\sigma m^2}{3D_\lambda}\frac{\partial T^4}{\partial r} \tag{2-13}$$

where

D_λ = extinction coefficient

σ = Stefan-Boltzmann constant

m = reflective index.

The equation (2-13) is non-linear. This non-linearity can be eliminated using the Taylor expansion for T^4 around T_∞. Neglecting the higher order terms in the expansion, the linearized form is obtained as

$$T^4 = 4T_\infty^{\,3} T - 3T_\infty^{\,4} \tag{2-14}$$

Substituting equation (2-14) into (2-13), the Rosseland approximation is expressed as

$$q_r = -\frac{16\sigma m^2}{3D_\lambda}\frac{\partial T}{\partial r} T_\infty^{\,3} \tag{2-15}$$

In the energy equation (2-5), the conduction heat transfer term and radiation heat transfer term may be expressed as

$$k\left(1+\frac{4}{3N}\right)\left(\frac{1}{r}\frac{\partial T}{\partial r}+\frac{\partial^2 T}{\partial r^2}\right) \tag{2-16}$$

where

$$N = \frac{kD_\lambda}{4\sigma m^2 T_\infty^3}\ , \quad \text{conduction to radiation ratio}$$

Using above equation, the energy equation becomes

$$v_r\frac{\partial T}{\partial r} + v_z\frac{\partial T}{\partial z} = \alpha\left(1+\frac{4}{3N}\right)\left(\frac{1}{r}\frac{\partial T}{\partial r}+\frac{\partial^2 T}{\partial r^2}\right) \tag{2-17}$$

By defining generalized Grashof and Prandtl numbers as

$$G_r = L^{(n+2)} \frac{\left\{g\beta\left(T_w - T_\infty\right)\right\}^{(2-n)}}{\nu^2}$$

and (2-18)

$$P_r = \nu^{(2/1+n)}\, L^{(1-n/1+n)} \frac{\left\{g\beta L\left(T_w - T_\infty\right)\right\}^{\frac{3(n-1)}{2(n+1)}}}{\alpha}$$

This relation of course can be reduced to the usual expressions for Newtonian fluids when $n = 1$.

Non-dimensional coordinates and velocities are expressed as

$$\begin{aligned} z^* &= \frac{z}{L} \\ r^* &= \frac{r}{L} G_r^{1/2(n+1)} \\ v_z^* &= \frac{v_z}{u_\circ} \\ v_r^* &= \frac{v_r}{u_\circ} G_r^{1/2(n+1)} \end{aligned} \qquad (2\text{-}19)$$

where

$$u_\circ = \sqrt{g\beta L\left(T_w - T_\infty\right)}$$

The continuity equation reduces to

$$\frac{\partial v_r^*}{\partial r^*} + \frac{1}{r^*} v_r^* + \frac{\partial v_z^*}{\partial z^*} = 0 \qquad (2\text{-}20)$$

The momentum equation reduces to

$$v_z^* \frac{\partial v_z^*}{\partial z^*} + v_r^* \frac{\partial v_z^*}{\partial r^*} = \frac{1}{r^*} \frac{\partial}{\partial r^*} \left\{ r^* \left(\frac{\partial v_z^*}{\partial r^*} \right)^n \right\} + \frac{T - T_\infty}{T_w - T_\infty} \qquad (2\text{-}21)$$

The energy equation reduces to

$$v_z^* \frac{\partial T}{\partial z^*} + v_r^* \frac{\partial T}{\partial r^*} = \frac{1}{\mathbf{P_r}}\left(1 + \frac{4}{3N}\right)\left(\frac{1}{r^*}\frac{\partial T}{\partial r^*} + \frac{\partial^2 T}{\partial r^{*2}}\right) \tag{2-22}$$

Let $\dfrac{T - T_\infty}{T_w - T_\infty} = \theta^*$.

The momentum equation becomes

$$v_z^* \frac{\partial v_z^*}{\partial z^*} + v_r^* \frac{\partial v_z^*}{\partial r^*} = \frac{1}{r^*}\frac{\partial}{\partial r^*}\left\{ r^* \left(\frac{\partial v_z^*}{\partial r^*}\right)^n \right\} + \theta^*. \tag{2-23}$$

The energy equation becomes

$$v_z^* \frac{\partial \theta^*}{\partial z^*} + v_r^* \frac{\partial \theta^*}{\partial r^*} = \frac{1}{\mathbf{P_r}}\left(1 + \frac{4}{3N}\right)\left(\frac{1}{r^*}\frac{\partial \theta^*}{\partial r^*} + \frac{\partial^2 \theta^*}{\partial r^{*2}}\right) \tag{2-24}$$

The boundary conditions are

for $r^* = r_o^*(z)$

$$v_r^* = 0 \tag{2-25}$$

$$v_z^* = 0$$

$$\theta^* = \theta_w^*(z)$$

for $r^* \rightarrow \infty$

$$v_z^* \rightarrow 0 \qquad (2\text{-}26)$$

$$\theta^* \rightarrow 0.$$

2.3 Similarity transformation

The stream function is defined by

$$v_r^* = -\frac{1}{r^*}\frac{\partial \psi^*}{\partial z^*}$$

$$v_z^* = \frac{1}{r^*}\frac{\partial \psi^*}{\partial r^*} \qquad (2\text{-}27)$$

In this study, a linear one-parameter group of transformation is chosen of the form.

$$z^* = A^{\alpha_1} z$$

$$r^* = A^{\alpha_2} r$$

$$\psi^* = A^{\alpha_3} \psi \qquad (2\text{-}28)$$

$$\theta^* = A^{\alpha_4} \theta$$

where

α_1, α_2, α_3 and α_4 = constants.

By using the definition of stream function ψ, the momentum equation is written as

$$\frac{1}{r^*}\frac{\partial \psi^*}{\partial r^*}\frac{\partial}{\partial z^*}\left(\frac{1}{r^*}\frac{\partial \psi^*}{\partial r^*}\right) - \frac{1}{r^*}\frac{\partial \psi^*}{\partial z^*}\frac{\partial}{\partial r^*}\left(\frac{1}{r^*}\frac{\partial \psi^*}{\partial r^*}\right) = \frac{1}{r^*}\frac{\partial}{\partial r^*}\left[r^* + \left\{\frac{\partial}{\partial r^*}\left(\frac{1}{r^*}\frac{\partial \psi^*}{\partial r^*}\right)\right\}^n\right] + \theta^*. \qquad (2\text{-}29)$$

The energy equation is written as

$$\frac{1}{r^*}\frac{\partial \psi^*}{\partial r^*}\frac{\partial \theta^*}{\partial z^*} - \frac{1}{r^*}\frac{\partial \psi^*}{\partial z^*}\frac{\partial \theta^*}{\partial r^*} = \frac{1}{P_r}\left(1+\frac{4}{3N}\right)\left(\frac{1}{r^*}\frac{\partial \theta^*}{\partial r^*} + \frac{\partial^2 \theta^*}{\partial r^{*2}}\right) \tag{2-30}$$

The boundary conditions (2-25) and (2-26) can be written as

for $r^* = r_o^*(z)$

$$\frac{\partial \psi^*}{\partial z^*} = 0$$

$$\frac{\partial \psi^*}{\partial r^*} = 0$$

$$\theta^* = \theta_w^*(z) \tag{2-31}$$

for $r^* \to \infty$

$$\frac{1}{r^*}\frac{\partial \psi^*}{\partial r^*} \to 0$$

$$\theta^* \to 0 \tag{2-32}$$

To obtain a similarity transformation for boundary layer equations, the linear group (2-27) will be employed. Then momentum equation (2-29) is transformed as

$$A^{(-\alpha_1 - 4\alpha_2 + 2\alpha_3)}\frac{1}{r}\frac{\partial \psi}{\partial r}\frac{\partial}{\partial z}\left(\frac{1}{r}\frac{\partial \psi}{\partial r}\right) - A^{(-\alpha_1 - 4\alpha_2 + 2\alpha_3)}\frac{1}{r}\frac{\partial \psi}{\partial z}\frac{\partial}{\partial r}\left(\frac{1}{r}\frac{\partial \psi}{\partial r}\right)$$

$$= A^{(-\alpha_2 - 3n\alpha_2 + n\alpha_3)}\frac{1}{r}\frac{\partial}{\partial r}\left[r + \left\{\frac{\partial}{\partial r}\left(\frac{1}{r}\frac{\partial \psi}{\partial r}\right)\right\}^n\right] + A^{\alpha_4}\theta. \tag{2-33}$$

The energy equation is transformed as

$$A^{(-\alpha_1 -2\alpha_2 +\alpha_3 +\alpha_4)} \frac{1}{r}\left(\frac{\partial\psi}{\partial r}\frac{\partial\theta}{\partial z} - \frac{\partial\psi}{\partial z}\frac{\partial\theta}{\partial r}\right) = A^{(-2\alpha_2+\alpha_4)} \frac{1}{\mathbf{P_r}}\left(1+\frac{4}{3N}\right)\left(\frac{1}{r}\frac{\partial\theta}{\partial r} + \frac{\partial^2\theta}{\partial r^2}\right) \tag{2-34}$$

In order to determine α_1, α_2, α_3 and α_4, the condition of invariancy is considered. Under this invariancy condition the power of transformation parameter A should be equal in equation (2-33) and (2-34), respectively.

By equating the powers of parameter A and solving the resulting equations, we can obtain the following equations.

$$\alpha_1 = \alpha_3$$
$$\alpha_1 = -4\alpha_2 + 2\alpha_3 - \alpha_4$$
$$(n-1)\,\alpha_1 = 3(n-1)\,\alpha_2$$

The constant n of the power-law type appears in a common coefficient of (n-1). Since this study focuses on non-Newtonian fluid ($n \neq 1$), it never happens that (n-1) equals zero. Therefore, the common term,(n-1), is cancelled.

Finally, the relations between the constants α_1, α_2, α_3 and α_4 are obtained as following.

$$\alpha_2 = \frac{1}{3}\alpha_1$$
$$\alpha_3 = \alpha_1 \tag{2-35}$$
$$\alpha_4 = -\frac{1}{3}\alpha_1$$

Next step is to seek "absolute invariants" under this group of transformations. Absolute invariants are functions having the same form before and after the transformations.

$$\eta_1 = rz^t = r^* z^{*t} = A^{(\alpha_1 t+\alpha_2)}\, rz^t.$$

By eliminating the parameter A, the absolute invariants can be obtained

$$\alpha_1 t + \alpha_2 = 0$$
$$t = -\frac{\alpha_2}{\alpha_1}$$

From equation (2-35) and above equation

$$t = -\frac{1}{3}$$

Hence

$$\eta_1 = rz^{-1/3} \qquad (2\text{-}36)$$

Hensen [15] showed that any power of an invariant is also an invariant under the same transformation. Therefore, the new invariant η will be obtained as a square of equation (2-36).

$$\eta = \left(rz^{-1/3}\right)^2 \qquad (2\text{-}37)$$

When r goes to $r_\circ$, η becomes $\eta_\circ$. Hence

$$\eta_\circ = \left(r_\circ z^{-1/3}\right)^2$$

This relation specified the shape of the needle. The shape of needle is restricted as

$$r_d(z) = \eta_\circ^{1/2} z^{1/3}$$

Using the same procedure, the similarity stream function and similarity temperature are given as

$$f(\eta) = \psi z^p = \psi^* z^{*p} = A^{(\alpha_1 p+\alpha_3)} \psi z^p$$

and

$$g(\eta) = \theta z^s = \theta^* z^{*s} = A^{(\alpha_1 s+\alpha_4)} \theta z^s.$$

By eliminating parameter A and using equation (2-35), the values of p and s are determined.

$$p = -1$$
$$s = \frac{1}{3}.$$

Hence

$$f(\eta) = \psi z^{-1} \qquad (2\text{-}38)$$

$$g(\eta) = \theta z^{1/3} \qquad (2\text{-}39)$$

Taking the partial derivative of the absolute invariant η with respect to r and z

$$\frac{\partial \eta}{\partial r} = 2rz^{-2/3}$$
$$\frac{\partial \eta}{\partial z} = -\frac{2}{3} r^2 z^{-5/3}$$

The following task is to express each of the terms in the momentum and energy equation in terms of η .

$$\begin{aligned}
\frac{\partial \psi}{\partial z} &= \frac{\partial}{\partial z}(z f) = f - \frac{2}{3} r^2 z^{-2/3} f' \\
\frac{\partial \psi}{\partial r} &= \frac{\partial}{\partial r}(z f) = 2rz^{1/3} f' \\
\frac{\partial^2 \psi}{\partial r^2} &= \frac{\partial}{\partial r}\left(\frac{\partial \psi}{\partial r}\right) = 2z^{1/3} f' + 4r^2 z^{-1/3} f'' \\
\frac{\partial^2 \psi}{\partial z \partial r} &= \frac{\partial}{\partial z}\left(\frac{\partial \psi}{\partial r}\right) = \frac{2}{3} rz^{-2/3} f' - \frac{4}{3} r^3 z^{-4/3} f'' \\
\frac{\partial \theta}{\partial z} &= \frac{\partial}{\partial z}(z^{-1/3} g) = -\frac{1}{3} z^{-4/3} g - \frac{2}{3} r^2 z^{-2} g' \\
\frac{\partial \theta}{\partial r} &= \frac{\partial}{\partial r}(z^{-1/3} g) = 2rz^{-1} g' \\
\frac{\partial^2 \theta}{\partial r^2} &= \frac{\partial}{\partial r}\left(\frac{\partial \theta}{\partial r}\right) = 2z^{-1} g' + 4r^2 z^{-5/3} g''
\end{aligned} \tag{2-40}$$

The momentum equation is transformed as

$$\text{Left Hand Side} = \frac{4}{3} rz^{-1/3} f'^2 - 4rz^{-1/3} f f'' \tag{2-41}$$

and

$$\text{Right Hand Side} = (4f'')^{(n-1)} (rz^{-1/3})^n \left\{ n\left(8\eta f''' + 4f''\right) + 4f'' \right\} + rz^{-1/3} g \tag{2-42}$$

From equation (2-41) and (2-42), the transformed momentum equation is obtained as

$$\left(4\eta^{1/2} f''\right)^{(n-1)} \left\{n\left(8\eta f''' + 4f''\right) + 4f''\right\} + 4ff'' - \frac{4}{3}f'^{2} + g = 0 . \tag{2-43}$$

The energy equation is transformed as

$$\text{Left Hand Side} = -\frac{2}{3} z^{-1} f'g - 2z^{-1} fg' \tag{2-44}$$

and

$$\text{Right Hand Side} = \frac{1}{P_r}\left(1 + \frac{4}{3N}\right)\left(4z^{-1} g' + 4\eta z^{-1} g''\right) \tag{2-45}$$

From equation (2-44) and (2-45), the transformed energy equation is obtained as

$$\eta g'' + g' + \frac{P_r}{6\left(1 + \frac{4}{3N}\right)}\left(f'g + 3fg'\right) = 0 . \tag{2-46}$$

When n = 1, the boundary layer equations reduce to the simple expression for Newtonian fluid. Also these equations for Newtonian fluid are exactly same as the equations, which are reported by T.Govindarajulu [5], for non-isothermal case ($n = -\frac{1}{3}$). This agrees with the fact, as reported by Acrivos [2], that the similarity solution does not exist for non-Newtonian power-law fluids ($n \neq 1$) in free convection over an isothermal surface.

The final step is to find the boundary conditions. The transformations, equations (2-37) - (2-39), show that similarity solutions exist only if

$$\theta_w(z) = z^{-1/3}.$$

Only with this term of $\theta_w(z)$ may constant boundary conditions be imposed on $f(\eta)$ and $g(\eta)$.

The boundary conditions are transformed to

for $\eta = \eta_o$

$$f(\eta) = 0$$
$$f'(\eta) = 0 \qquad (2\text{-}47)$$
$$g(\eta) = 1$$

for $\eta \to \infty$

$$f'(\eta) \to 0$$
$$g(\eta) \to 0. \qquad (2\text{-}48)$$

CHAPTER III

ANALYSIS OF THE SIMILARITY SOLUTION

3.1 Satisfaction of the asymptotic boundary conditions

The solution of similarity equations derived in the previous chapter is considered. The similarity equations for non-Newtonian natural convection with radiation effect are rearranged as

$$f''' = -\frac{1}{n\eta}\left\{\left(\frac{n+1}{2}\right)f'' + \left(4\eta^{1/2}\right)^{(1-n)}\left(\frac{1}{2}ff''^{(2-n)} - \frac{1}{6}f'^{2}f''^{(1-n)} + \frac{1}{8}gf''^{(1-n)}\right)\right\} \tag{2-43a}$$

and

$$g'' = -\frac{1}{\eta}\left\{g' + \frac{p_r}{6\left(1+\frac{4}{3N}\right)}\left(f'g + 3fg'\right)\right\} \tag{2-46a}$$

for $\eta = \eta_o$

$$\begin{aligned} f(\eta) &= 0 \\ f'(\eta) &= 0 \\ g(\eta) &= 1 \end{aligned} \tag{2-47}$$

for $\eta \to \infty$

$$\begin{aligned} f'(\eta) &= 0 \\ g(\eta) &= 0\,. \end{aligned} \tag{2-48}$$

Since the above equations are highly non-linear, it is almost impossible to solve them analytically. Furthermore, there are not enough boundary conditions to determine all the constants of integration even if one could obtain a value $f(\eta)$ and $g(\eta)$ in an analytical

form. Even though these difficulties exist in the solution of these similarity equations, we can obtain good results by using numerical techniques.

The numerical integration of the ordinary differential equations of boundary layer theory involves the satisfaction of asymptotic boundary conditions; that is, some boundary conditions are specified as limits that must be approached at large values of the independent variable corresponding to the edge of the boundary layer. In order to integrate the differential equations numerically from the wall to the edge of the boundary layer, it is necessary to specify as many additional conditions at the wall as there are conditions to be satisfied at the edge of the boundary layer. These additional initial conditions have to be varied in order to satisfy the conditions at the edge of the boundary layer.

Nachtsheum and Swigert [16] provided a method for predicting the amount of error in initial guess for the starting values used in the numerical solution of differential equations which include asymptotic boundary conditions. Knowledge of the magnitude of this error allows adjustment of the initial guesses depending on the limits of accuracy for the desired problem. This technique is employed in our boundary layer problem. When η goes to infinity, the boundary conditions are expressed as

$$\begin{aligned} \lim_{\eta \to \infty} f'(\eta) &= 0 \\ \lim_{\eta \to \infty} g(\eta) &= 0 \end{aligned} \qquad (3\text{-}1)$$

These asymptotic boundary conditions are replaced by the conditions that $f'(\eta) = 0$ and $g(\eta) = 0$ at some specific value of η_{edge} where the edge of the boundary layer occurs. Hence the equation (3-1) is replaced as

$$f'(\eta_{edge}) = 0$$
$$g(\eta_{edge}) = 0 \qquad (3\text{-}2)$$

The given boundary value problem is equivalent to the problem of finding values of $f''(\eta_\circ)$ and $g'(\eta_\circ)$ for which the boundary condition at the edge of the boundary layer are satisfied.

$$f'_{edge}\left[f''(\eta_\circ)\right] = 0$$
$$g_{edge}\left[g'(\eta_\circ)\right] = 0 \qquad (3\text{-}3)$$

where

$$f'_{edge} = f'(\eta_{edge}), \quad g_{edge} = g(\eta_{edge}).$$

The functions $f'_{edge}\left[f''(\eta_\circ)\right]$ and $g_{edge}\left[g'(\eta_\circ)\right]$ in this problem are not, in general, explicit. They will be expressed as functions of $f''(\eta_\circ)$ and $g'(\eta_\circ)$ through an integration of equation (2-43) and (2-46), respectively. If the initial guesses are expressed as

$$f''(\eta_\circ) = h \qquad (3\text{-}4)$$
$$g'(\eta_\circ) = w, \qquad (3\text{-}5)$$

then the small changes Δh in h and Δw in w change f' and g by the amount

$$\frac{\partial f'}{\partial h}\Delta h \text{ and } \frac{\partial g}{\partial w}\Delta w.$$

Thus the correction to an approximation of the boundary condition for given initial guesses can be obtained by the linear equation.

$$f' + f'_h \Delta h + f'_w \Delta w = 0 \tag{3-6}$$

$$g + g_h \Delta h + g_w \Delta w = 0 \qquad \text{at } \eta = \eta_{edge} \tag{3-7}$$

where

$$f'_h = \frac{\partial f'}{\partial h}\ , \quad f'_w = \frac{\partial f'}{\partial w}\ , \text{ etc.}$$

The preceding equations have to be supplemented by the following equations to satisfy the asymptotic boundary conditions.

$$f'' + f''_h \Delta h + f''_w \Delta w = 0 \tag{3-8}$$

$$g' + g'_h \Delta h + g'_w \Delta w = 0 \tag{3-9}$$

where

$$f''_h = \frac{\partial f''}{\partial h}\ , \quad f''_w = \frac{\partial f''}{\partial w}\ , \text{ etc.}$$

A satisfactory solution that is consistent with the idea that the boundary conditions can not be satisfied exactly at a finite value of η is to seek the least-squares error solution of above equations (3-6) - (3-9). Therefore, the discrepancies will be considered as

$$\delta_1 = f' + f'_h \Delta h + f'_w \Delta w \tag{3-10}$$

$$\delta_2 = g + g_h \Delta h + g_w \Delta w \tag{3-11}$$

$$\delta_3 = f'' + f''_h \Delta h + f''_w \Delta w \tag{3-12}$$

$$\delta_4 = g' + g'_h \Delta h + g'_w \Delta w \qquad \text{at } \eta = \eta_{edge} \tag{3-13}$$

where

δ_1, δ_2, δ_3 and δ_4 are arbitrary close to zero.

Δh and Δw can be obtained for the above equations which make the sum $\delta_1^2+\delta_2^2+\delta_3^2+\delta_4^2$ as small as possible. This can be accomplished by differentiating

$\delta_1^2+\delta_2^2+\delta_3^2+\delta_4^2$ with respect to Δh and Δw respectively and equating the result to zero. This least-squares error solution for those quantities is given by the solution of the following matrix equation;

$$\begin{pmatrix} f_h'^2 + g_h^2 + f_h''^2 + g_h'^2 & f_h' f_w' + g_h g_w + f_h'' f_w'' + g_h' g_w' \\ f_h' f_w' + g_h g_w + f_h'' f_w'' + g_h' g_w' & f_w'^2 + g_w^2 + f_w''^2 + g_w'^2 \end{pmatrix} \begin{pmatrix} \Delta h \\ \Delta w \end{pmatrix}$$

$$= -\begin{pmatrix} f' f_h' + g g_h + f'' f_h'' + g' g_h' \\ f' f_w' + g g_w + f'' f_w'' + g' g_w' \end{pmatrix} \qquad (3\text{-}14)$$

The value of h and w that give $\Delta h = \Delta w = 0$ correspond to the minimum with respect to h and w of the quantity

$$E = f'^2 + g^2 + f''^2 + g'^2 \quad \text{at } \eta = \eta_{edge} \qquad (3\text{-}15)$$

The partial derivatives with respect to h and w that appear in equation (3-14) are obtained by integrating the appropriate perturbation differential equations. The perturbation differential equations for the h derivatives are

$$f_h''' = -\frac{1}{n\eta}\left[\left(\frac{n+1}{2}\right)f_h'' + \left(4\eta^{1/2}\right)^{(1-n)}\left\{\frac{1}{2}\left(f_h f''^{(2-n)} + (2-n) f f''^{(1-n)} f_h''\right)\right.\right.$$

$$\left.\left. - \frac{1}{6}\left((1-n) f_h'' f'^2 f''^{(-n)} + 2 f' f_h' f''^{(1-n)}\right) + \frac{1}{8}\left(g_h f''^{(1-n)} + (1-n) f''^{(-n)} f_h'' g\right)\right\}\right] \qquad (3\text{-}16)$$

and

$$g_h'' = -\frac{1}{\eta}\left\{ g_h' + \frac{P_r}{6\left(1+\frac{4}{3N}\right)}\left(f_h' g + f' g_h + 3 f_h g' + 3 f g_h' \right) \right\} \tag{3-17}$$

with the initial condition

at $\eta = \eta_o$

$$\begin{aligned} f_h(\eta) &= 0 \\ f_h'(\eta) &= 0 \\ f_h''(\eta) &= 1 \\ g_h(\eta) &= 0 \\ g_h'(\eta) &= 0 . \end{aligned} \tag{3-18}$$

The perturbation equations for w derivatives are

$$f_w''' = -\frac{1}{n\eta}\left[\left(\frac{n+1}{2}\right) f_w'' + \left(4\eta^{1/2}\right)^{(1-n)} \left\{ \frac{1}{2}\left(f_w f^{''(2-n)} + (2-n) f f^{''(1-n)} f_w'' \right) \right.\right.$$

$$\left.\left. - \frac{1}{6}\left((1-n) f_w'' f'^2 f^{''(-n)} + 2 f' f_w' f^{''(1-n)} \right) + \frac{1}{8}\left(g_w f^{''(1-n)} + (1-n) f^{''(-n)} f_w'' g \right) \right\} \right] \tag{3-19}$$

and

$$g_w'' = -\frac{1}{\eta}\left\{ g_w' + \frac{P_r}{6\left(1+\frac{4}{3N}\right)}\left(f_w' g + f' g_w + 3 f_w g' + 3 f g_w' \right) \right\} \tag{3-20}$$

with the initial conditions

at $\eta = \eta_\circ$

$$f_w(\eta) = 0$$
$$f_w'(\eta) = 0$$
$$f_w''(\eta) = 0 \qquad (3\text{-}21)$$
$$g_w(\eta) = 0$$
$$g_w'(\eta) = 1 .$$

Note that the equations for w derivatives are the same as the equations for h derivatives. However, the integrals of these equations will be different since the initial conditions are different.

3.2 Results of the solution algorithm

The method used by Nachtsheum and Swigert was selected to solve the differential equations. This method appears to be insensitive to initial guesses and converges quickly to the solution. This technique was successfully applied to obtain numerical values of the transformed equations. The algorithm has been incorporated into a computer program which calculates the solutions out to a point η_{edge} where the corrections to the initial guesses for $f''(\eta_\circ)$ and $g'(\eta_\circ)$ are calculated. The deviations of f' and g from the asymptotic values are checked at η_{edge}. If the calculated error is greater than the prescribed value, the magnitude of η_{edge} is increased and new initial guesses for $f''(\eta_\circ)$ and $g'(\eta_\circ)$ are used to solve the equations until the boundary conditions and error limits are met.

The integration was performed at η_{edge} which was an assumed end of the boundary layer. The initial guess used for η_{edge} was 4.0 which was increased by a small increment

dx until convergence was achieved and the required error criterion was met. In the present study, the small increment dx varies from 0.05 to 0.002 and the maximum error ranges from 0.1×10^{-2} to 0.5×10^{-4} according to various values of the Prandtl number and the needle shape parameter $\eta_\circ$. The values of the small increment dx, maximum error and needle shape parameter for various Prandtl numbers were listed in the Table 1. The initial guesses for $f''(\eta_\circ)$ and $g'(\eta_\circ)$ were 1.0 and -0.5, respectively. In numerical calculations this created a confusion for the machine since the computer could not handle a negative base raised to a non-integer power resulting in a complex variable. However, this problem was successfully handled by identifying real and imaginary parts and choosing the real part as the solution. For example, let's consider $y^{0.9}$ where y is an arbitrary real number. When y is a positive real number, this calculation can be handled by the computer without any difficulties. However, when y is a negative real number the computer sometimes does

Table 1. The values of the needle shape parameter $\eta_\circ$, dx, and the maximum error according to different Prandtl numbers.

Pr	$\eta_\circ$	dx	E_{max}
100	0.1	0.05	0.5×10^{-4}
	0.001	0.002	0.1×10^{-3}
10	0.1	0.05	0.1×10^{-3}
	0.001	0.002	0.5×10^{-3}
1	0.1	0.05	0.1×10^{-2}
	0.001	0.002	0.1×10^{-2}

not know what to do about the negative number raised to a non-integer power. To avoid this difficulty we can modify $y^{0.9}$ as follows:

$$y^{0.9} = |y|^{0.9} \times (-1)^{0.9} \tag{3-22}$$

where

y is a negative real number.

The first term of the right-hand-side in the equation (3-22) can be calculated by computer because the base is a positive real number. The problem remains in the second term of the right-hand-side. By using Euler's formula, it is expressed as

$$(-1)^{0.9} = e^{0.9\pi i} = \cos(0.9\pi) + i \times \sin(0.9\pi) \tag{3-23}$$

From equation (3-22) and (3-23)

$$y^{0.9} = |y|^{0.9} \times \left\{\cos(0.9\pi) + i \times \sin(0.9\pi)\right\}. \tag{3-24}$$

Equation (3-24) consists of real and imaginary parts. The imaginary part can be neglected in the calculation since the entire solution is based on real values. Therefore,

$$y^{0.9} = |y|^{0.9} \times \cos(0.9\pi). \tag{3-25}$$

Fig.2 through Fig.21 show the results of the solution. Some typical velocity profiles and temperature profiles for different values of n at various conduction-to-radiation ratio parameters N and the Prandtl numbers are shown in Fig.2 through Fig.7. It can be observed that an increase in the Prandtl number produces decreased momentum and thermal boundary layer thicknesses. The Prandtl number is defined as the ratio of the kinetic viscosity to the thermal diffusivity. Therefore, the Prandtl number provides a measure of the relative effectiveness of momentum and energy transport by diffusion in the velocity

and thermal boundary layers, respectively. The value of the Prandtl number strongly influences the relative growth of the velocity and thermal boundary layers. If the Prandtl number is near unity, the momentum boundary layer and the thermal boundary layer are comparable. For oils, the Prandtl number is greater than 1 and the momentum boundary layer becomes larger than the the thermal boundary layer. The opposite is true for a liquid metal, for which the Prandtl number is less than 1. From Fig.2 - Fig.7 we can compare the momentum boundary layer with the thermal boundary layer in different non-Newtonian power-law fluids as well as in the Newtonian fluid. Those results agree with above interpretation.

The influence of the conduction-to-radiation ratio parameters, N, is also clearly revealed. If the conduction-to-radiation ratio parameters, N, approach infinity, the convection effect is dominant while the radiation effect is negligible. On the other hand, the radiation effect is dominant when the conduction-to-radiation ratio parameters, N, go to zero. For dominant radiation effects, the thickness of momentum and thermal boundary layers increase. Previous research [17] reported that an increased degree of radiation increases the thermal and velocity boundary layers in Newtonian fluids. A similar conclusion holds for non-Newtonian fluids, as seen from Fig.8 through Fig.13.

Results of the velocity and temperature profiles for different needle sizes and for non-Newtonian flow behavior index, n, ranging from 0.8 to 1.2 are shown in Fig.14 through Fig.21. First, it is noted that the flow behavior index n has a significant effect. For a given needle size, the velocity profile for n=1.2 is much steeper than that for n=1.0 and 0.8. Secondly, a progressive decrease in the needle size results in increased heat transfer rates and skin friction at a given the Prandtl number and conduction-to-radiation ratio parameters, N.

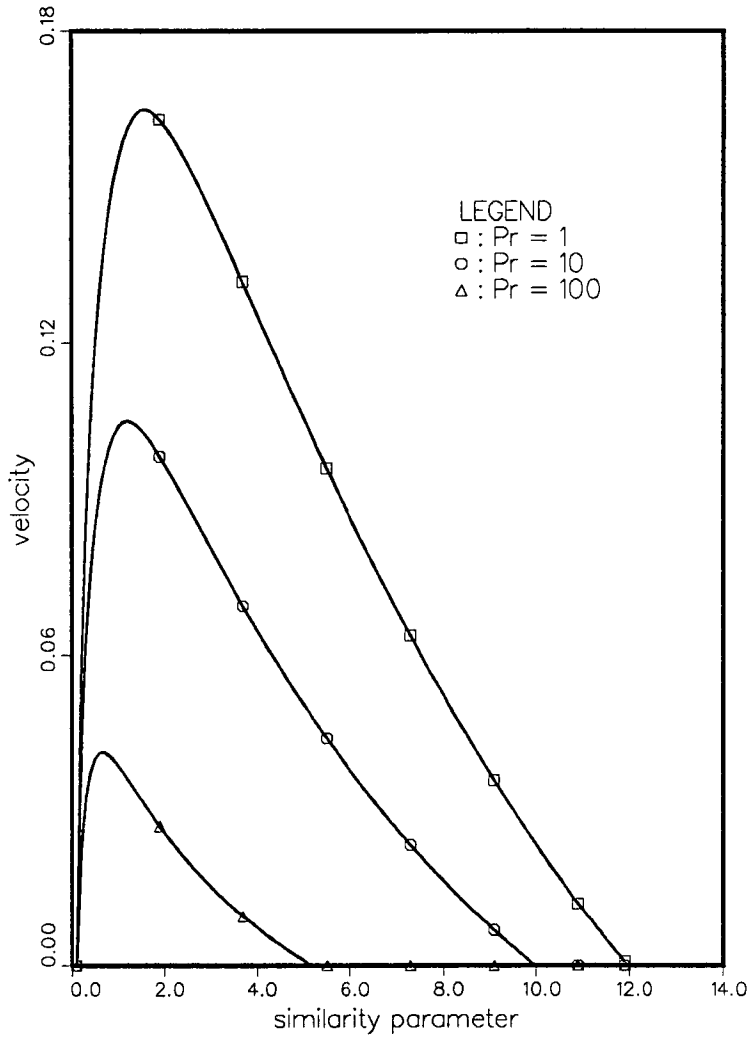

Fig.2. Similarity velocity profile with η_o = 0.1 and no radiation in non-Newtonian fluid (n = 1.2)

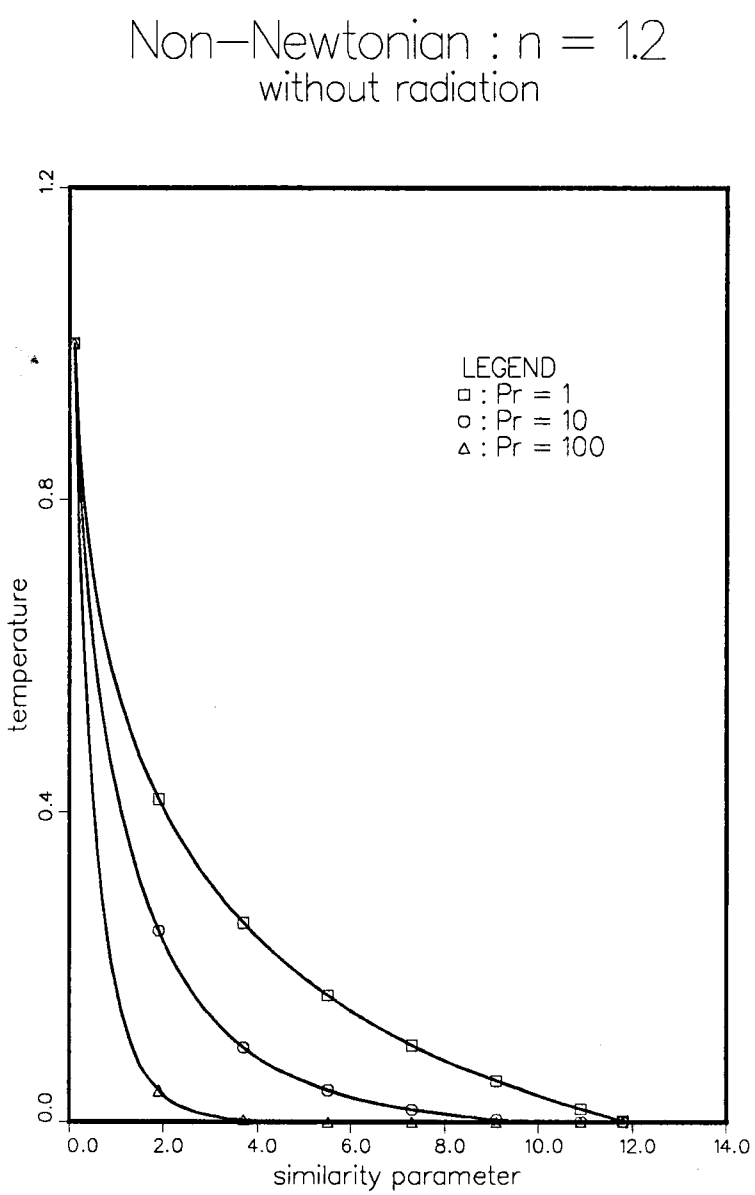

Fig.3. Similarity temperature profile with η_o = 0.1 and no radiation in non-Newtonian fluid (n = 1.2)

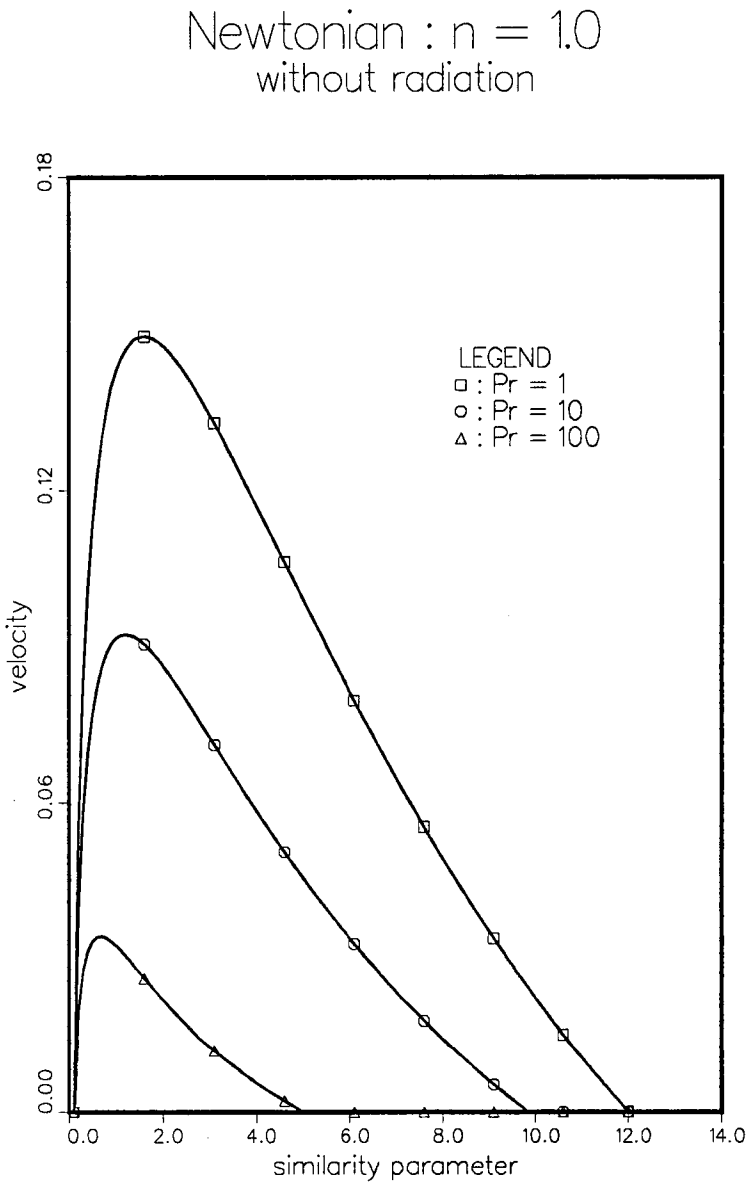

Fig.4. Similarity velocity profile with η_o = 0.1 and no radiation in Newtonian fluid (n = 1.0)

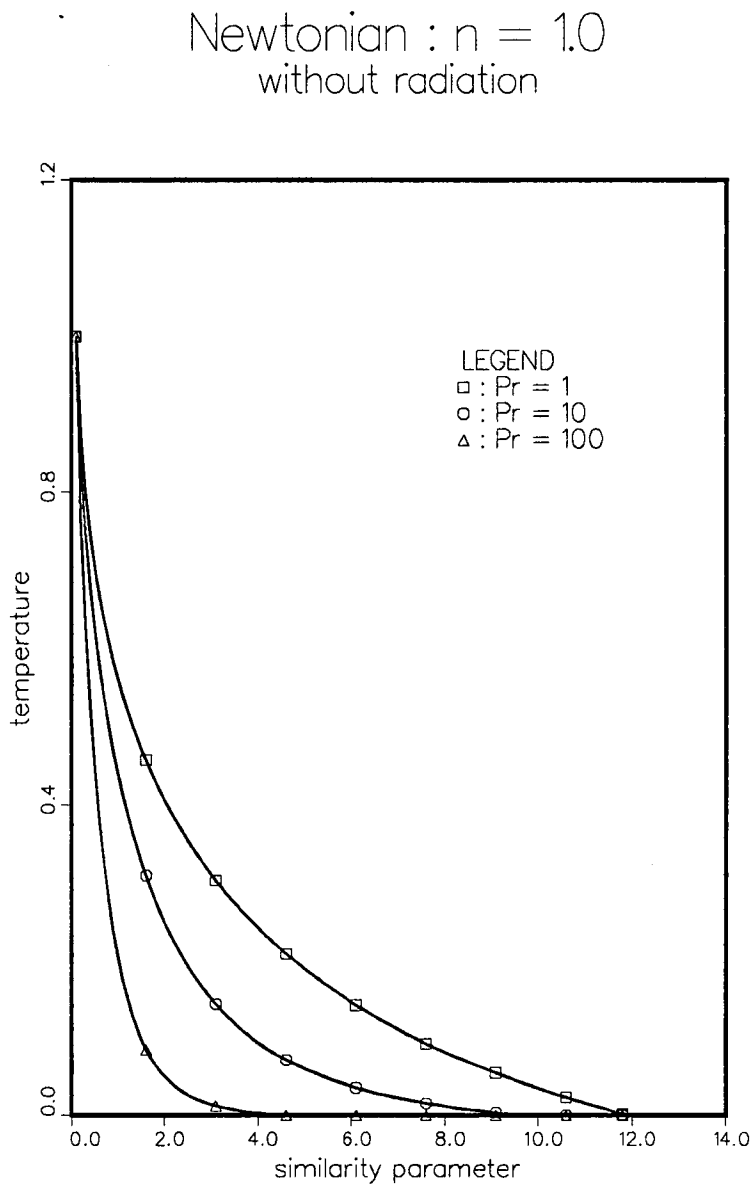

Fig.5. Similarity temperature profile with η_o = 0.1 and no radiation in Newtonian fluid (n = 1.0)

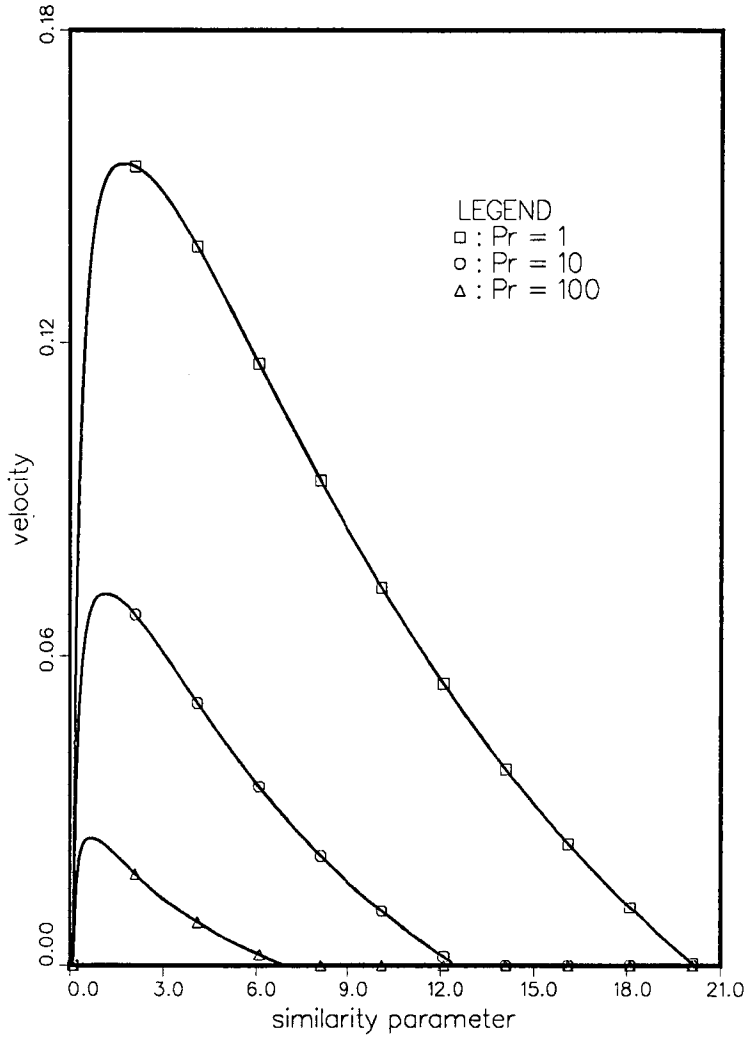

Fig.6. Similarity velocity profile with η_o = 0.1 and no radiation in non-Newtonian fluid (n = 0.8)

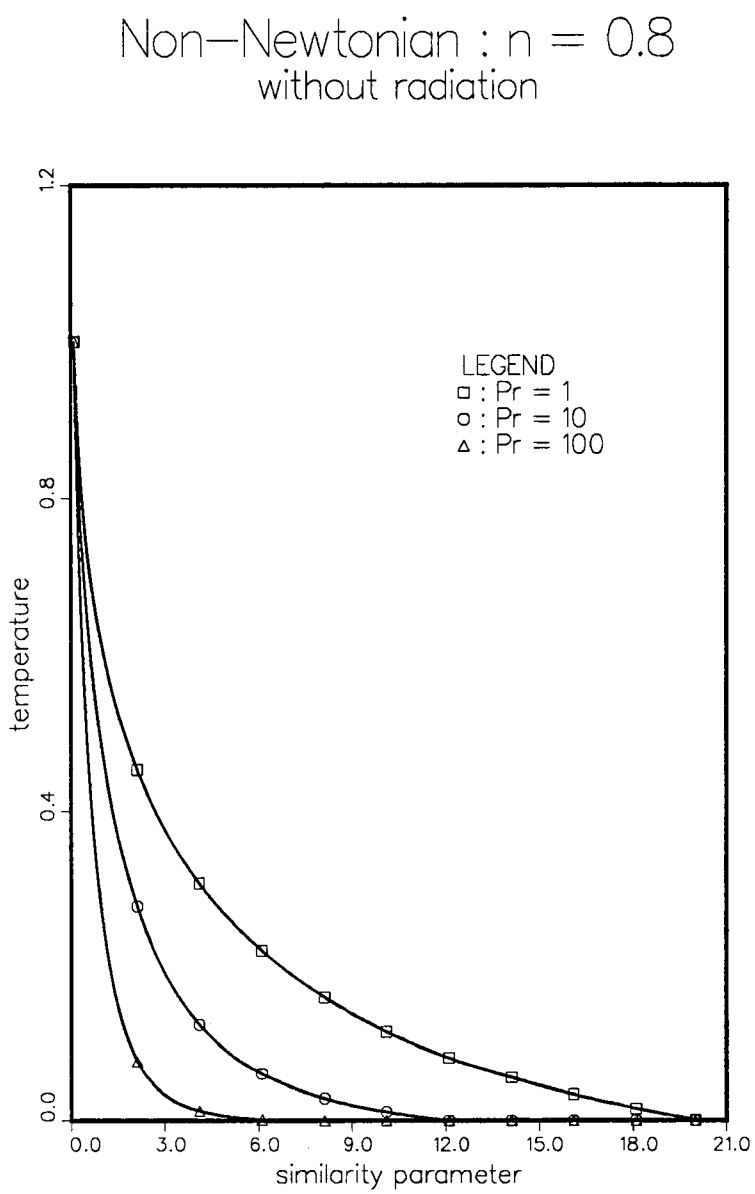

Fig.7. Similarity temperature profile with η_o = 0.1 and no radiation in non-Newtonian fluid (n = 0.8)

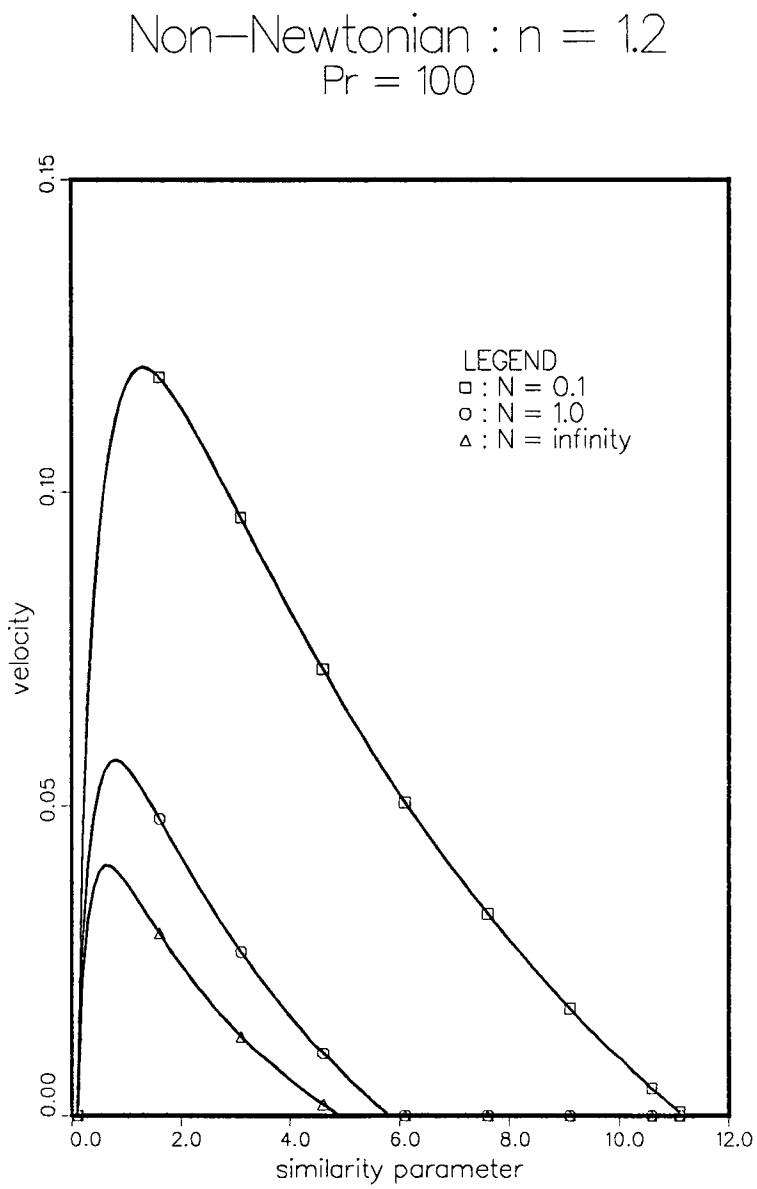

Fig.8. Similarity velocity profile with η_o = 0.1 and Pr = 100 in non-Newtonian fluid (n = 1.2)

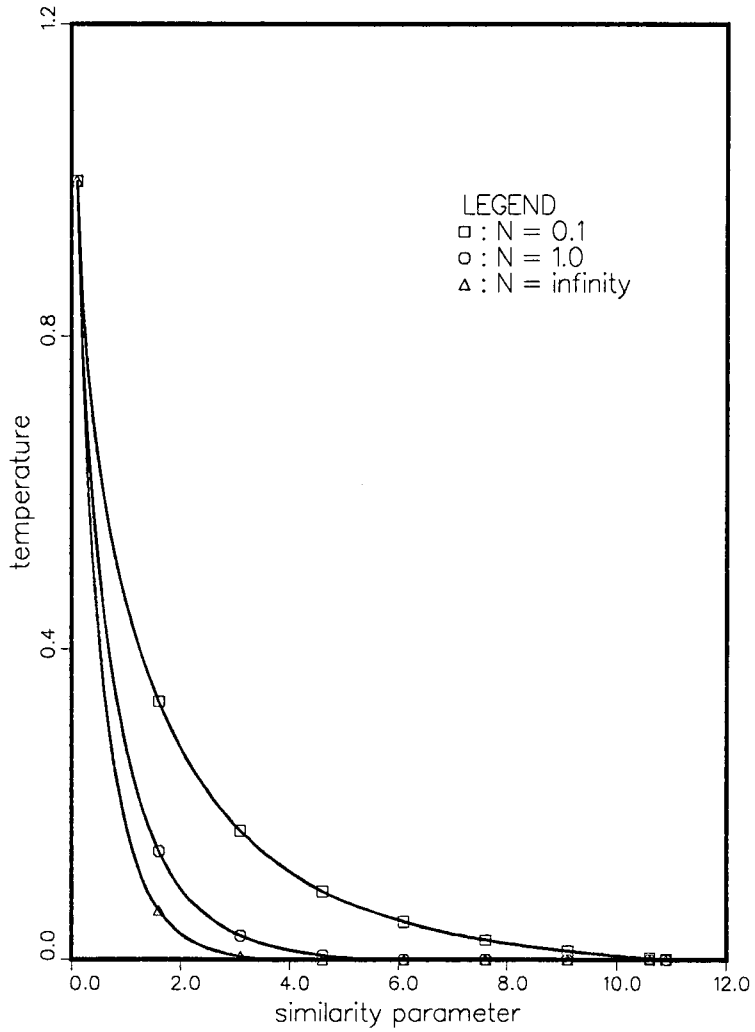

Fig.9. Similarity temperature profile with η_o = 0.1 and Pr = 100 in non-Newtonian fluid (n = 1.2)

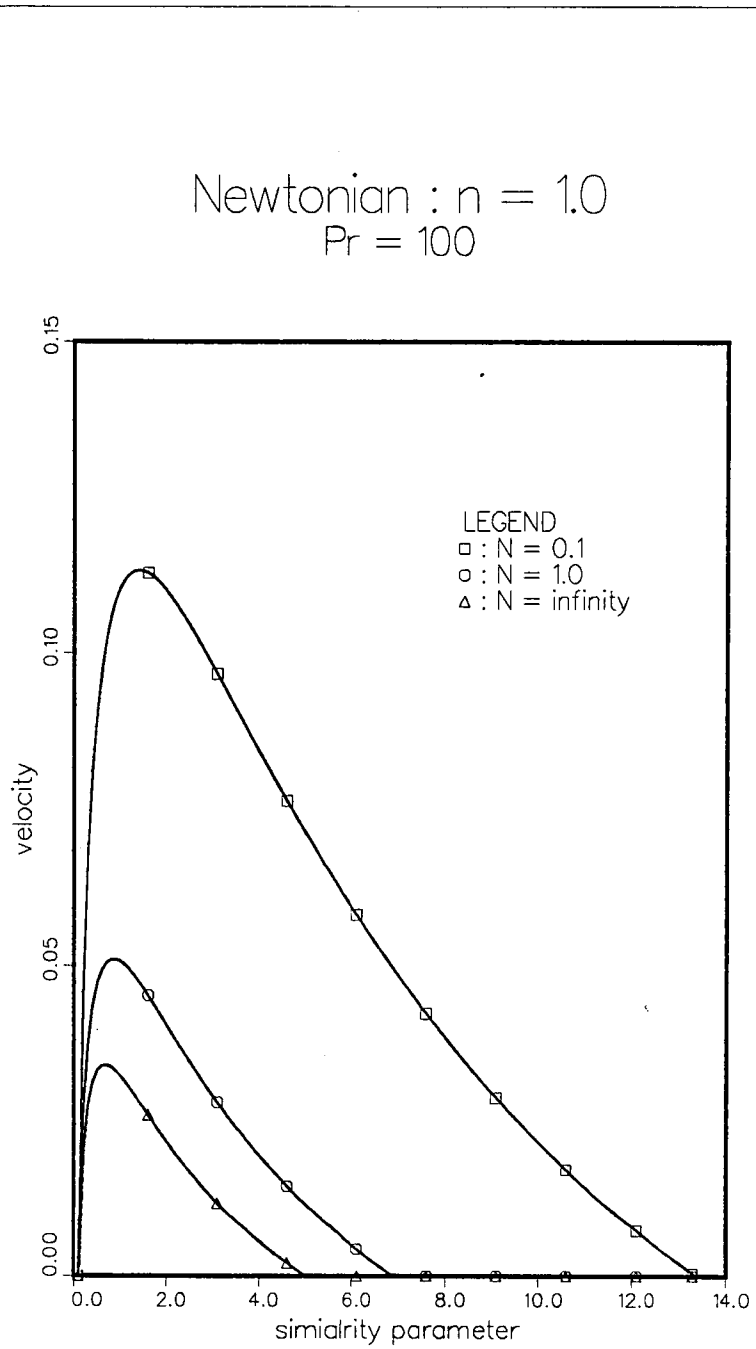

Fig.10. Similarity velocity profile with η_o = 0.1 and Pr = 100 in Newtonian fluid (n = 1.0)

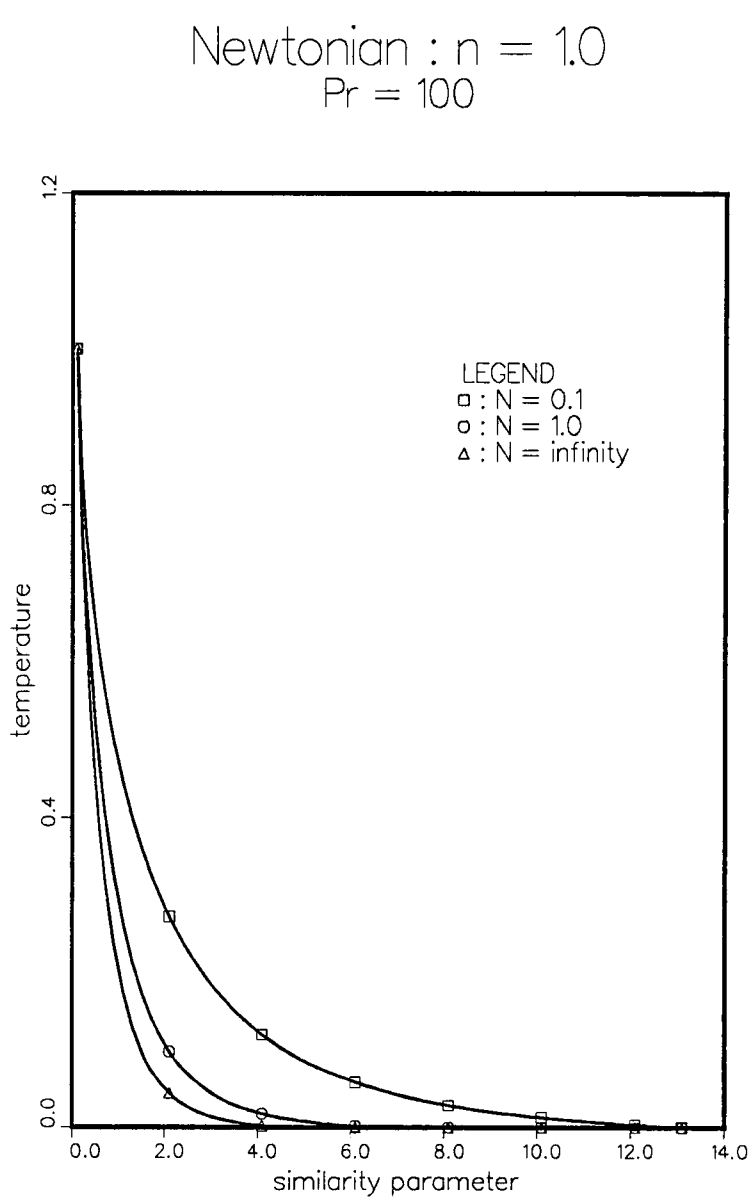

Fig.11. Similarity temperature profile with η_o = 0.1 and Pr = 100 in Newtonian fluid (n = 1.0)

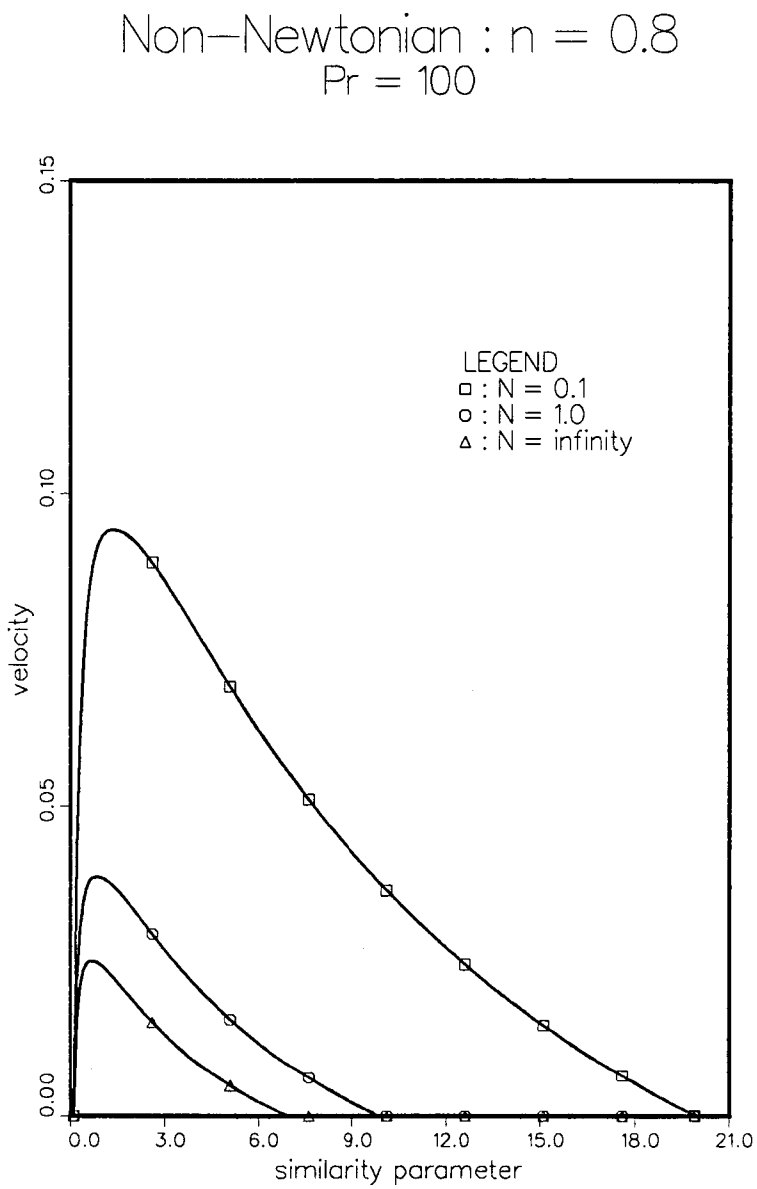

Fig.12. Similarity velocity profile with η_o = 0.1 and Pr = 100 in non-Newtonian fluid (n = 0.8)

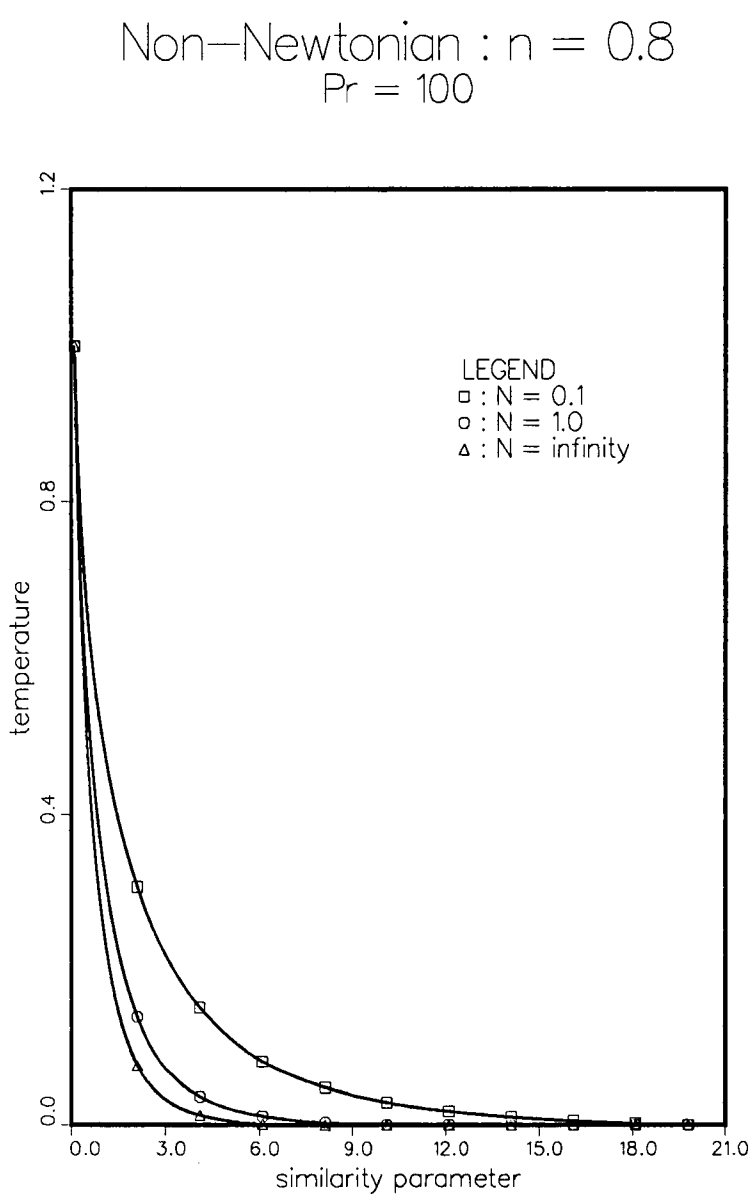

Fig.13. Similarity temperature profile with η_o = 0.1 and Pr = 100 in non-Newtonian fluid (n = 0.8)

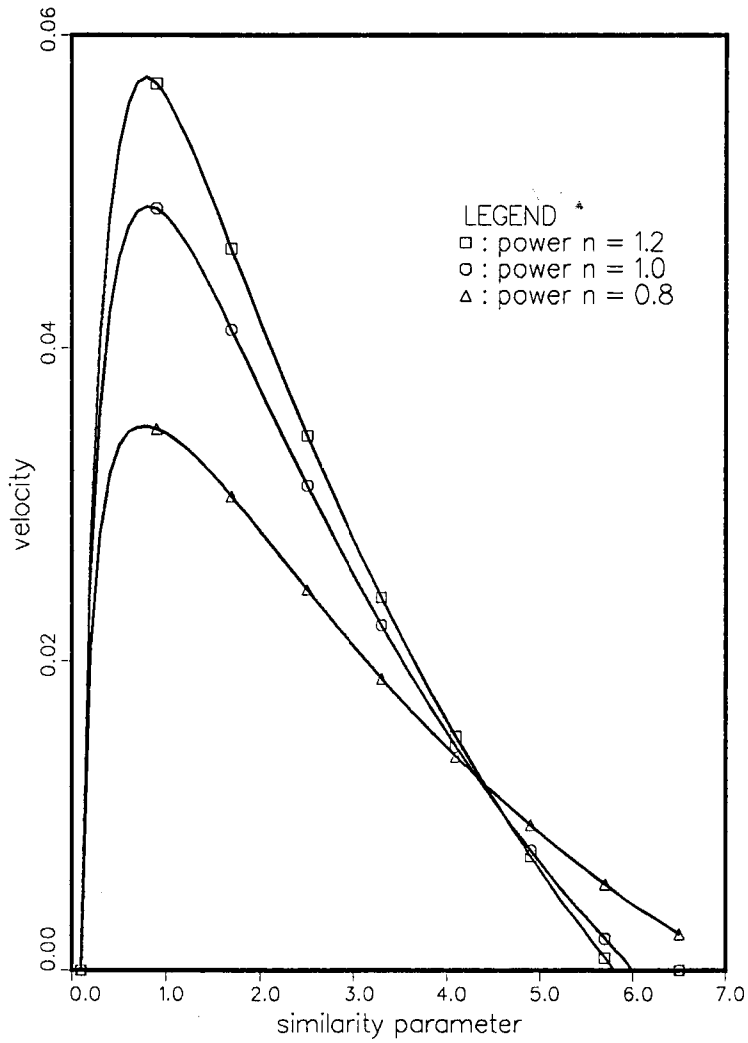

Fig.14. Similarity velocity profile with η_o = 0.1, Pr = 100 and radiation effect (N = 1.0)

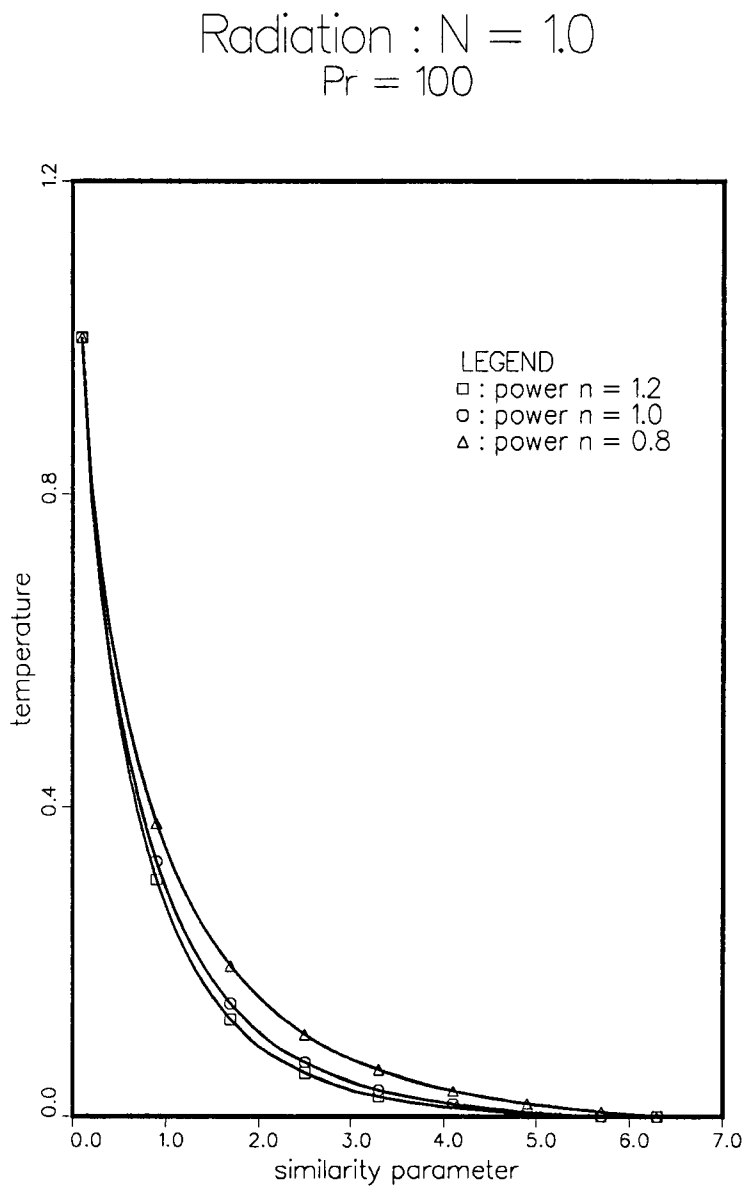

Fig.15. Similarity temperature profile with η_o = 0.1, Pr = 100 and radiation effect (N = 1.0)

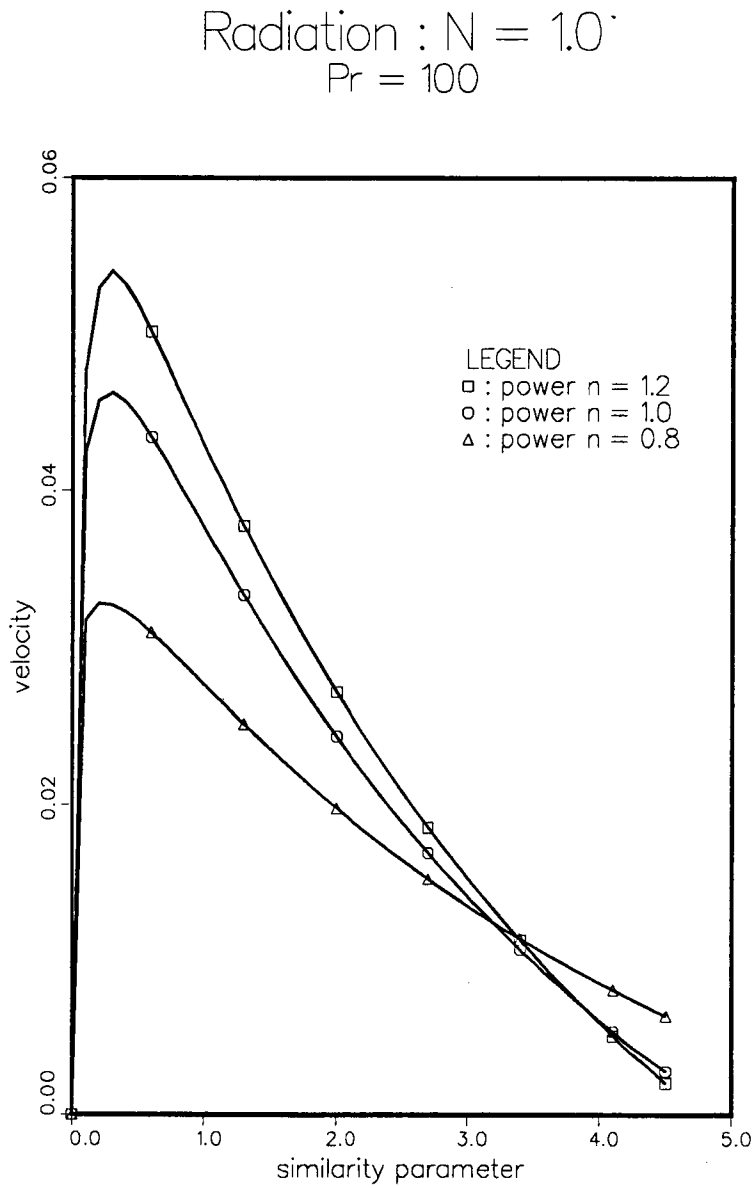

Fig.16. Similarity velocity profile with η_o = 0.001, Pr = 100 and radiation effect (N = 1.0)

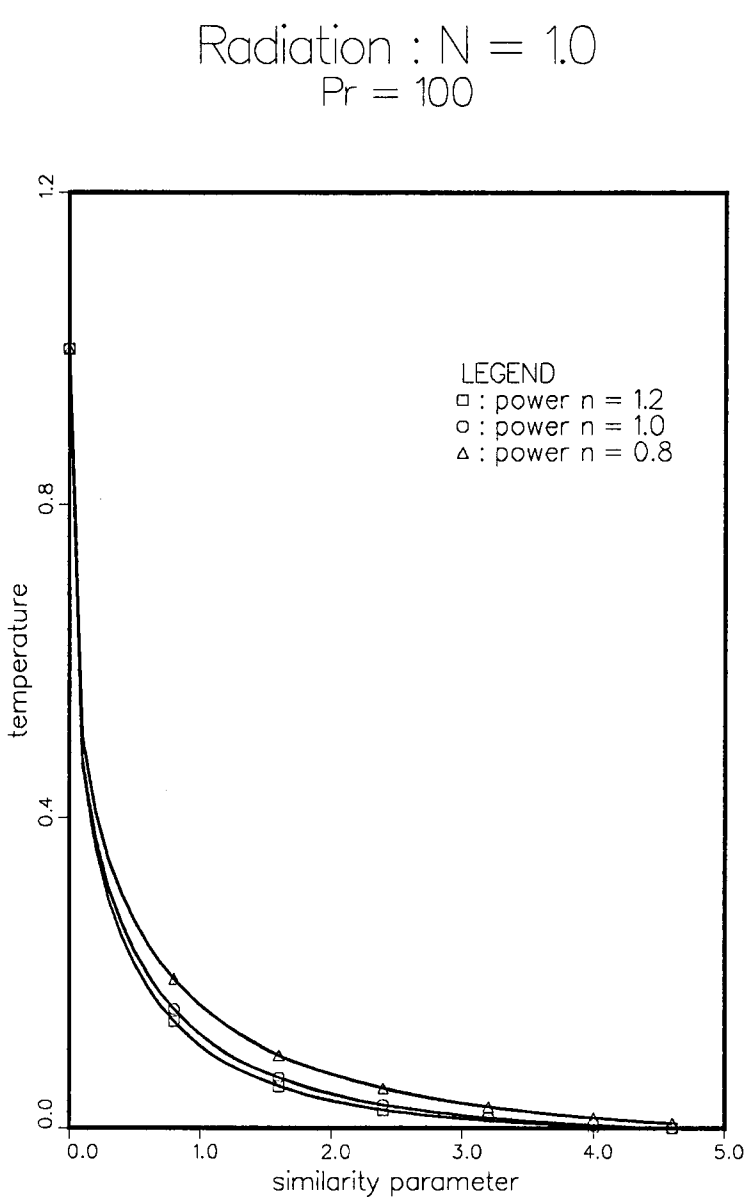

Fig.17. Similarity temperature profile with η_∞ = 0.001, Pr = 100 and radiation effect (N = 1.0)

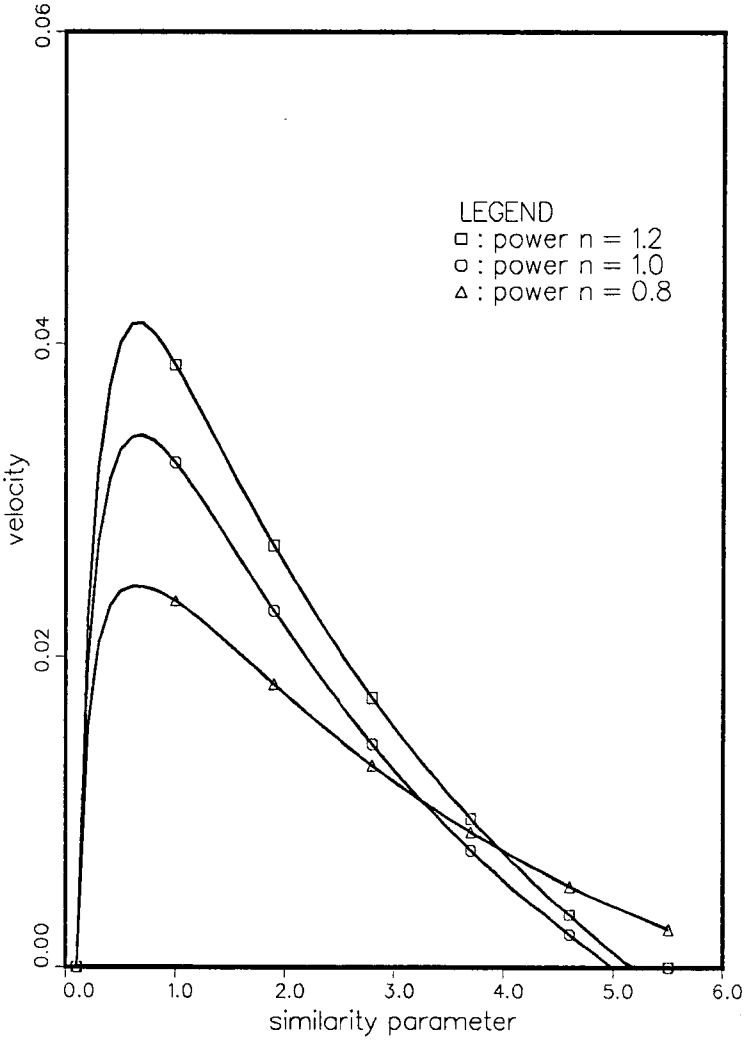

Fig.18. Similarity velocity profile with η_o = 0.1, Pr = 100 and no radiation (N = infinity)

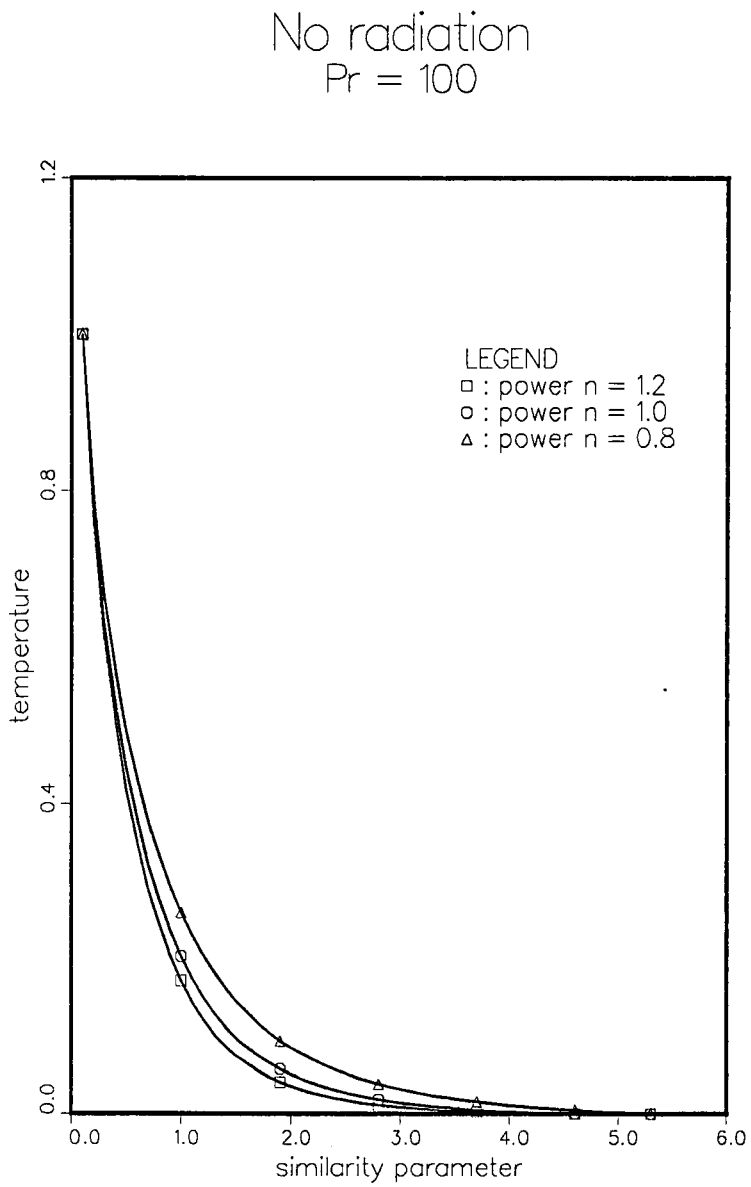

Fig.19. Similarity temperature profile with η_o = 0.1, Pr = 100 and no radiation (N = infinity)

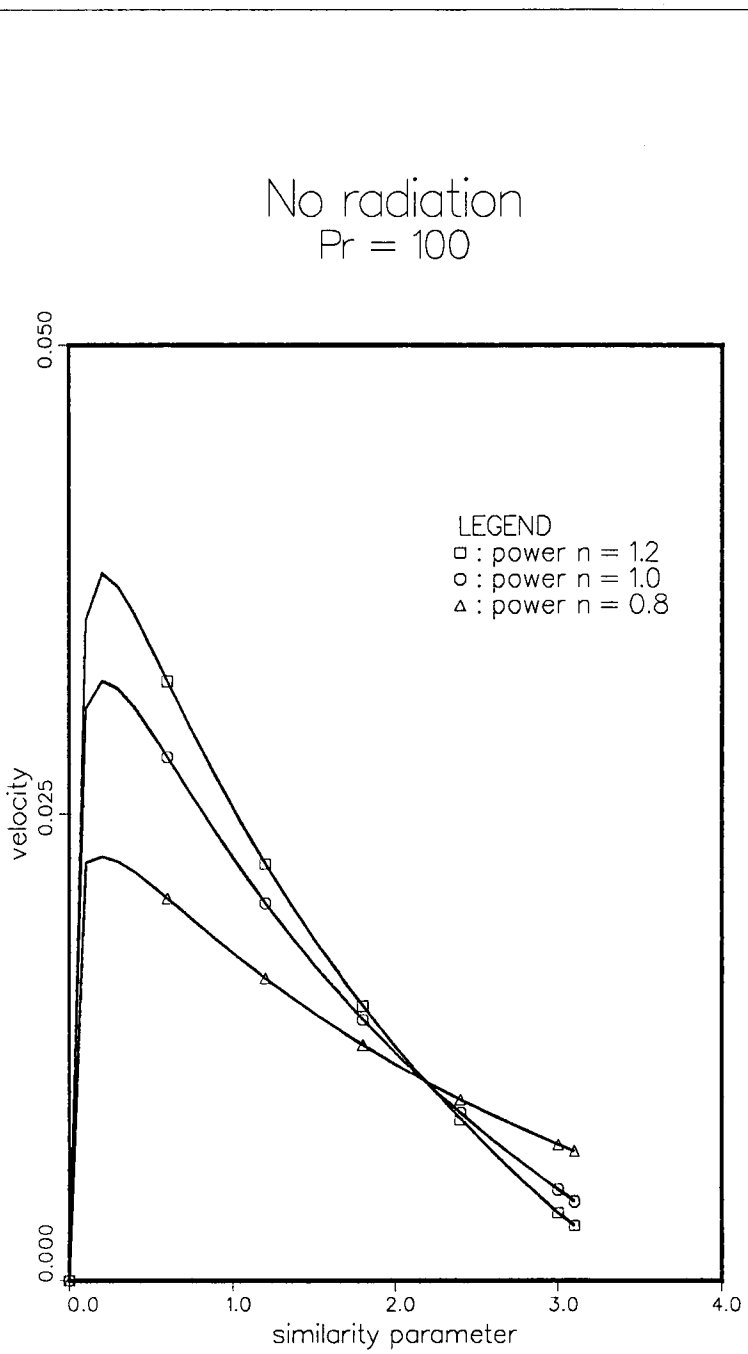

Fig.20. Similarity velocity profile with η_o = 0.001, Pr = 100 and no radiation (N = infinity)

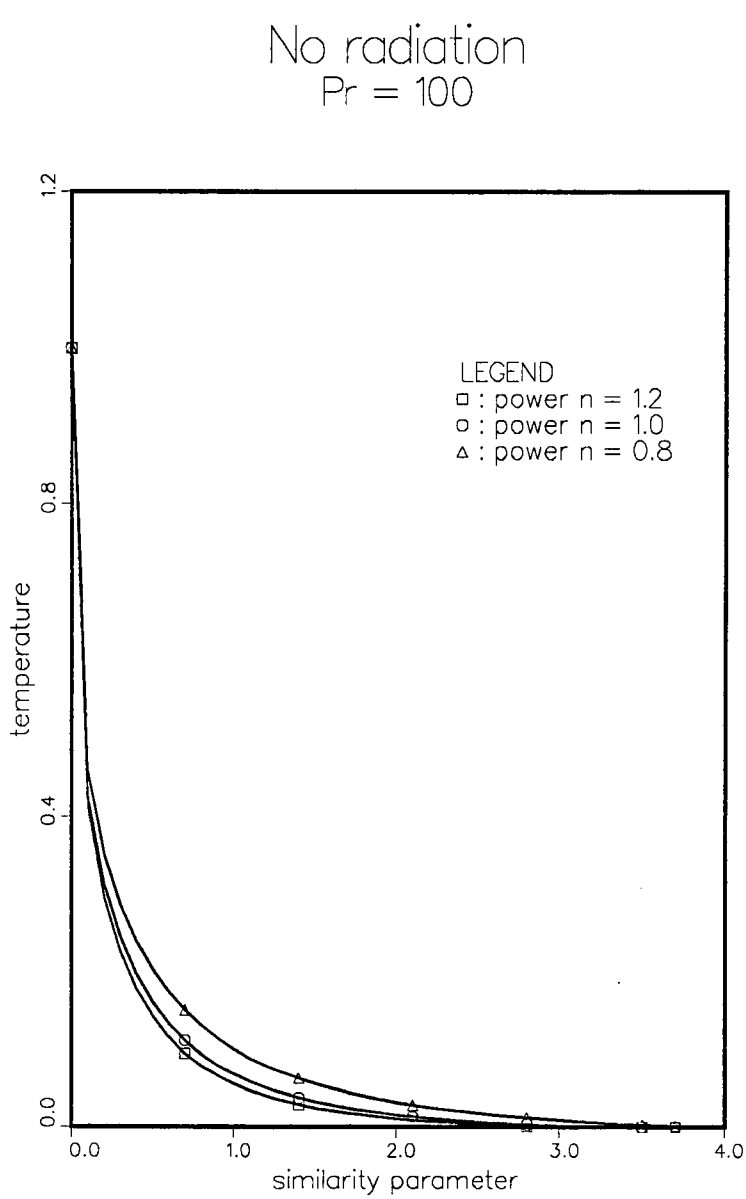

Fig.21. Similarity temperature profile with η_o = 0.001, Pr = 100 and no radiation (N = infinity)

CHAPTER IV

CONCLUSIONS AND RECOMMENDATIONS

The theoretical considerations of this study provide information which can be used to examine a laminar boundary layer flow under the influence of natural convection and radiation heat transfer.

This study showed the feature of non-Newtonian power-law fluids and the effects of thermal radiation on laminar natural convection, as well as the influence of the needle shape. The set of boundary layer equations were reduced to the ordinary differential forms of the momentum and energy equations by using the one linear parameter group theory. The radiative heat flux term in the energy equation was simplified by the use of the Rosseland approximation for optically thick medium. By using the Taylor expansion method, the temperature term was linearized. The momentum and energy equations were obtained by using the Runge-Kutta-perturbation method which gave corrections to initial guesses for the slop of the velocity and temperature profiles. As noted earlier the results for the needle sizes and for n ranging from 0.8 to 1.2 with different conduction-to-radiation parameter N and Prandtl numbers were shown in Fig.2 through Fig.21. From those results, we can make the following conclusions:

1. The influences of the Prandtl number are remarkable. The physical interpretation of the Prandtl number follows from its definition as a ratio of the momentum diffusivity to the thermal diffusivity. High Prandtl number means that the momentum diffusion rate greatly exceeds the energy diffusion. For a given fluid, as the Prandtl number was increased, the skin friction decreased while the heat transfer rate increased.

2. The momentum and thermal boundary layer thickness of the non-Newtonian power-law fluid increases as the radiation heat transfer becomes more dominant. This shows that as the radiation heat transfer becomes dominant, the heat distribution becomes more spread out in the fluid boundary layer. This phenomenon in non-Newtonian fluid is similar to that in Newtonian fluids.

3. The properties of non-Newtonian power-law fluid have profound effects on flows along thin needles. For a given needle size and Prandtl number, the velocity and energy profile for a dilatant fluid is steeper than that for Newtonian and pseudo-plastic fluids. However, this conclusion should be taken cautiously due to the lack of data at other non-Newtonian values.

4. The effects of transverse curvature of the needle on non-Newtonian flow are of significance. For a given fluid, the more slender the needle, the thinner the boundary layer thickness.

5. The needle shape affects both the skin friction and the heat transfer rate. As the needle became more slender, the skin friction and the heat transfer rate were increased for a given fluid.

6. Finally, we note the physical insights obtained through this study may be useful in temperature fields for which needle-shaped probes are used. This study showed properties of non-Newtonian power law-fluids while the non-Newtonian behavior indices, n are near unity. It is recommended to study further for the wide ranges of n.

LIST OF REFERENCES

LIST OF REFERENCES

1. Lee,S.Y., and Ames,W.F., "Similarity solutions for non-Newtonian fluids", A.I.Ch.E. Journal, pp. 700-708, July 1966.

2. Acrivos,A., Shah,M.J., and Pertersen,E.E., "Momentum and heat transfer in laminar boundary-layer flows of non-Newtonian fluids past external surfaces", A.I.Ch.E. Journal, pp. 312-317, June 1960.

3.Schowalter,W.R., "The application of boundary-layer theory to power-law pseudoplastic fluids: similar solutions", A.I.Ch.E. Journal, pp. 24, 1960.

4. Cebeci,T. and Na,Y., "Laminar free-convection heat transfer from a needle", The Physics of Fluids, pp. 463-465, February 1969.

5. Govindarajulu,T., "Laminar free-convection heat transfer from a needle", The Physics of Fluids, pp. 211-212, January 1972.

6. Narain,J.P., and Uberoi,M.S., "Laminar free convection from vertical thin needles", The Physics of Fluids, pp. 928-929, May 1972.

7. Chen,J.L.S., "Natural convection from needles with variable wall temperature", ASME Paper, no. 80-HT-72, 1980.

8. Chen,J.L.S., "Natural convection from needles with variable wall heat flux", Journal of Heat Transfer, pp. 403-406, May 1983.

9. Viskata,R., and Grosh,R.J., "Boundary layer in thermal radiation absorbing and emitting media", Int. J. Heat Mass Transfer, vol.5, pp.795-806, 1962.

10. Novotny,J.L., and Yang,K.T., "The interaction of thermal radiation in optically thick boundary layers", ASME Paper, no.67-HT-9, 1967.

11. Goulard,R., "The transition from black body to Rosseland formulations in optically thick flows", Int. J. Heat Mass Transfer, vol.7, pp. 1145-1146, 1964.

12. Kim,K.H., Ozisik,M.N., and Mulligan,J.C., "A non-similar solution of heat transfer in external non-Newtonian flow with thermal radiation", AIAA Paper, no.73-116, 1973.

13. Kim,K.H., and Ozisik,M.N., "Application of normal-mode-expansion technique to absorbing, emitting and scattering point boundary layer flow", Development on Theoretical and Applied Mechanics, Vol. 10, pp. 681.

14. Galuska,M.J., and Kim,K.H., "Laminar natural convection heat transfer to non-Newtonian fluids with thermal radiation effects", Master Thesis, The University of Tennessee, 1982.

15. Hensen,A.G., "Similarity analysis of boundary value problems in engineering", Prentice Hall: Englewood Cliffs, NJ, 1964.

16. Nachtsheum,P.R., and Swigert,P., "Satisfaction of asymptotic boundary conditions in numerical solution of systems of non-linear equations of boundary layer type", NASA Technical Note D3004, National Aeronautics and Space Administration, 1965.

17. Lee,G.H., and Kim,K.H., "Laminar natural convection heat transfer along a needle with thermal radiation", Master Thesis, The University of Tennessee, 1987.

18. Incropera,F.P., and De Witt,D.P., "Fundamentals of Heat and Mass Transfer", 2nd eds., Wiley-Interscience, New York, 1981.

19. Ozisik,M.N., "Radiation transfer and interactions with conduction and convection", Wiley-Interscience, New York, 1973.

20. Siegel,R., and Howell,J.R., "Thermal radiation heat transfer", 2nd eds., Hemisphere Publishing Corporation, New York, 1981.

APPENDIX

```
      program vertical needle

*...  non-newtonian needle problem with radiation

*...  variables

      implicit real*8(a-h, o-z), integer (i-n)
      dimension ys(50),y(50),q(50)
      common/paramt/pn,rn,gw,pr


*...  open file

      open (unit=1,file='na9.dat',status='new')

*...  input the data

      pnn=0.1d+00
      pn =1.2
      pr =100.d0
      t1 =0.1d+00
      emax=0.1d-03
      gw=1.d0
      dzmax=0.1d+01
      dwmax=0.1d+01
      n=15
      ndnf=40
      dx=0.5d-01
      ndxw=2
      nf=2
      z=1.d0
      w=-5.d0
      isfw=0
      rn=4.d0/(3.d0*pnn)

      write(1,198) pn, emax, dx,pr,t1,pnn
      write(*,198) pn, emax, dx,pr,t1,pnn
198   format(3x,'pn=',f7.3,2x,'emax=',d10.3,2x,'dx=',f7.4,
     +       2x,'pr=',f7.3,2x,'xs=',f6.3,2x,'pnn=',f3.1//)

      write(1,55)
      write(*,55)
55    format(4x,'x',10x,'f',13x,'df',12x,'ddf',12x,'g',
     +       12x,'dg',/)

1     xs=t1
      ys(1)=0.d0
      ys(2)=0.d0
      ys(3)=z
      ys(4)=gw
```

```
        ys(5)=w
        ys(6)=0.d0
        ys(7)=0.d0
        ys(8)=1.d0
        ys(9)=0.d0
        ys(10)=0.d0
        ys(11)=0.d0
        ys(12)=0.d0
        ys(13)=0.d0
        ys(14)=0.d0
        ys(15)=1.d0

        if (isfw-5) 34,34,200
200     write(*,201) xs,ys(1),ys(2),ys(3),ys(4),ys(5)
        write(1,201) xs,ys(1),ys(2),ys(3),ys(4),ys(5)
201     format(1x,f6.3, 5(d14.6))

34      isr=0
        inf=1

3       call rnktgl(n,isr,xs,dx,ndxw,ys,xfc,y,q)

        if (isfw-5) 45,45,300
300     write(*,201) xfc,y(1),y(2),y(3),y(4),y(5)
        write(1,201) xfc,y(1),y(2),y(3),y(4),y(5)

45      if(inf-ndnf) 4,5,5
4       inf=inf+1
        isr=isr+1
        go to 3

5       a1= y(7)**2 + y(9)**2 + y(8)**2 + y(10)**2
        b1= y(7)*y(12)+y(9)*y(14)+y(8)*y(13)+y(10)*y(15)
        c1= -(y(2)*y(7)+y(4)*y(9)+y(3)*y(8)+y(5)*y(10))
        a2= b1
        b2= y(12)**2 + y(14)**2 + y(13)**2 + y(15)**2
        c2= -(y(2)*y(12)+y(4)*y(14)+y(3)*y(13)+y(5)*y(15))

        det= a1*b2 - b1*a2
        dz= (c1*b2 - b1*c2)/det
        dw= (a1*c2 - c1*b1)/det
        e = y(2)**2 + y(3)**2 + y(4)**2 + y(5)**2
        z = z+dz
        w = w+dw

        if (dabs(dz/z) .gt. dzmax .or. dabs(dw/w)
     +      .gt. dwmax) go to 1
        if ( e-emax) 13,14,14

14      ndnf=ndnf+nf
```

```
        go to 1
13      if (isfw-5) 401,401,402
401     isfw=isfw+10
        z=z-dz
        w=w-dw
        go to 1

402     write(*,203) e
        write(1,203) e
203     format(3x,'e=',d16.8)
800     continue
        stop
        end


*.....................................................


        subroutine rnktgl (n,isr,xs,dx,ndxw,ys,xfc,y,q)

        implicit real*8(a-h,o-z), integer(i-n)
        dimension ys(50), f(50), y(50), q(50)
        common/paramt/pn,rn,gw,pr


        a1=0.5d+00
        a2=0.1d+01-dsqrt(0.5d+00)
        a3=0.1d+01+dsqrt(0.5d+00)
        a4=0.1d+01/0.6d+01

        if(isr) 1,1,3
1       x=xs
        do 2 i=1,n
         y(i)=ys(i)
         q(i)=0.d0
2       continue

3       idx=1

5       call fnlist(x,y,f)

        do 10 i=1,n
         dk1=dx*f(i)
         y(i)=y(i) + a1*(dk1-0.2d+01*q(i))
         q(i)=q(i) + 0.3d+01*a1*(dk1-0.2d+01*q(i))-a1*dk1
10      continue

        x=x + 0.5d+00*dx
```

```
      call fnlist(x,y,f)

      do 20 i=1,n
       dk2=dx*f(i)
       y(i)=y(i) + a2*(dk2-q(i))
       q(i)=q(i) + 0.3d+01*a2*(dk2-q(i)) - a2*dk2
20    continue

      call fnlist(x,y,f)

      do 30 i=1,n
       dk3=dx*f(i)
       y(i)=y(i) + a3*(dk3-q(I))
       q(i)=q(i) + 0.3d+01*a3*(dk3-q(i)) - a3*dk3
30    continue

      x=x + 0.5d+00*dx

      call fnlist(x,y,f)

      do 40 i=1,n
       dk4=dx*f(i)
       y(i)=y(i) + a4*(dk4-0.2d+01*q(i))
       q(i)=q(i) + 0.3d+01*a4*(dk4-0.2d+01*q(i))-a4*dk4
40    continue

      if (idx-ndxw) 41,42,42
41    idx=idx+1
      go to 5
42    xfc=x

      return
      end


*.....................................................


      subroutine fnlist(x,y,f)

      implicit real*8(a-h,o-z), integer(i-n)
      dimension y(50), f(50)
      common/paramt/pn,rn,gw,pr


      rnn=1.d0 + rn
      sum1=1.d0-pn
      sum2=2.d0-pn
      sum3=sum1/2.d0
      pi=3.141592d+00
```

```
      f(1)=y(2)
      f(2)=y(3)
      if (y(3) .gt. 0.0d+00) go to 100
      if (y(3) .lt. 0.0d+00) go to 200
      if (y(3) .eq. 0.0d+00) go to 300
100   f(3)=-((pn+1)*y(3)/2.d0+x**(sum3)*4.d0**(sum1)*
     +      (y(1)*y(3)**(sum2)/2.d0-y(2)**2*y(3)**
     +      (sum1)/6.d0+y(4)*y(3)**(sum1)/8.d0))/(pn*x)
      go to 400
200   yy1=(cos(sum1*3.141592d+00))*(-y(3))**sum1
      yy2=(cos(sum2*3.141592d+00))*(-y(3))**sum2
      f(3)=-((pn+1)*y(3)/2.d0 + x**(sum3)*4.d0**(sum1)*
     +      (y(1)*yy2/2.d0-y(2)**2*yy1/6.d0+y(4)*yy1/
     +       8.d0))/(pn*x)
      go to 400
300   f(3)=0.0d+00
      go to 400
400   f(4)=y(5)
      f(5)=-(y(5)+(pr/(6.d0*rnn))*(y(2)*y(4)+3.d0*y(1)*
     +       y(5)))/x
      f(6)=y(7)
      f(7)=y(8)
      if (y(3) .gt. 0.0d+00) go to 500
      if (y(3) .lt. 0.0d+00) go to 600
      if (y(3) .eq. 0.0d+00) go to 700
500   f(8)=-((pn+1)*y(8)/2.d0+x**(sum3)*4.d0**(sum1)*
     +       ((y(6)*y(3)**(sum2)+(sum2)*y(1)*y(3)**
     +       (sum1)*y(8))/2.d0-((sum1)*y(3)**(-pn)*
     +       y(8)*y(2)**2+2.d0*y(3)**(sum1)*y(2)*y(7))
     +       /6.d0+(y(9)*y(3)**(sum1)+(sum1)*y(3)**
     +       (-pn)*y(8)*y(4))/8.d0))/(pn*x)
      go to 800
600   ss1=(cos(sum1*3.141592d+00))*(-y(3))**sum1
      ss2=(cos(sum2*3.141592d+00))*(-y(3))**sum2
      ss3=(cos(-pn*3.141592d+00))*(-y(3))**(-pn)
      f(8)=-((pn+1)*y(8)/2.d0+x**(sum3)*4.d0**(sum1)*
     +       ((y(6)*ss2 + (sum2)*y(1)*ss1*y(8))/2.d0-
     +       ((sum1)*ss3*y(8)*y(2)**2 + 2.d0*ss1*y(2)*
     +       y(7))/6.d0+(y(9)*ss1+(sum1)*ss3*y(8)*y(4))
     +       /8.d0))/(pn*x)
      go to 800
700   f(8)=-((pn+1)*y(8)/2.d0)/(pn*x)
      go to 800
800   f(9)=y(10)
      f(10)=-(y(10)+(pr/(6.d0*rnn))*(y(7)*y(4)+y(2)*y(9)+
     +        3.d0*y(6)*y(5) + 3.d0*y(1)*y(10)))/x
      f(11)=y(12)
      f(12)=y(13)
      if (y(3) .gt. 0.0d+00) go to 900
      if (y(3) .lt. 0.0d+00) go to 1000
      if (y(3) .eq. 0.0d+00) go to 1100
```

```
900     f(13)=-((pn+1)*y(13)/2.d0 + x**(sum3)*4.d0**(sum1)*
     +          ((y(11)*y(3)**(sum2)+(sum2)*y(1)*y(3)**
     +          (sum1)*y(13))/2.d0 - ((sum1)*y(3)**(-pn)*
     +         y(13)*y(2)**2+2.d0*y(3)**(sum1)*y(2)*y(12))/
     +          6.d0+(y(14)*y(3)**(sum1)+(sum1)*y(3)**(-pn)*
     +         y(13)*y(4))/8.d0))/(pn*x)
        go to 1200
1000    vv1=(cos(sum1*3.141592d+00))*(-y(3))**sum1
        vv2=(cos(sum2*3.141592d+00))*(-y(3))**sum2
        vv3=(cos(-pn*3.141592d+00))*(-y(3))**(-pn)
        f(13)=-((pn+1)*y(13)/2.d0+x**(sum3)*4.d0**(sum1)*
     +          ((y(11)*vv2 + (sum2)*y(1)*vv1*y(13))/2.d0-
     +          ((sum1)*vv3*y(13)*y(2)**2 + 2.d0*vv1*y(2)*
     +           y(12))/6.d0+(y(14)*vv1 + (sum1)*vv3*y(13)*
     +           y(4))/8.d0))/(pn*x)
        go to 1200
1100    f(13)=-((pn+1)*y(13)/2.d0)/(pn*x)
        go to 1200
1200    f(14)=y(15)
        f(15)=-(y(15)+(pr/(6.d0*rnn))*(y(12)*y(4)+y(2)*
     +          y(14)+3.d0*y(11)*y(5)+3.d0*y(1)*y(15)))/x


        return
        end
```

```
      program vertical needle

*...  non-newtonian needle problem without radiation

*...  variables

      implicit real*8(a-h, o-z), integer (i-n)
      dimension ys(50),y(50),q(50)
      common/paramt/pn,rn,gw,pr


*...  open file

      open (unit=1,file='na9.dat',status='new')

*...  input the data

      pn =1.2
      pr =100.d0
      t1 =0.1d+00
      emax=0.1d-03
      gw=1.d0
      dzmax=0.1d+01
      dwmax=0.1d+01
      n=15
      ndnf=40
      dx=0.5d-01
      ndxw=2
      nf=2
      z=1.d0
      w=-5.d0
      isfw=0

      write(1,198) pn, emax, dx,pr,t1,pnn
      write(*,198) pn, emax, dx,pr,t1,pnn
198   format(3x,'pn=',f7.3,2x,'emax=',d10.3,2x,'dx=',f7.4,
     +       2x,'pr=',f7.3,2x,'xs=',f6.3,2x,'pnn=',f3.1//)

      write(1,55)
      write(*,55)
55    format(4x,'x',10x,'f',13x,'df',12x,'ddf',12x,'g',
     +       12x,'dg',/)

1     xs=t1
      ys(1)=0.d0
      ys(2)=0.d0
      ys(3)=z
      ys(4)=gw
```

```
      ys(5)=w
      ys(6)=0.d0
      ys(7)=0.d0
      ys(8)=1.d0
      ys(9)=0.d0
      ys(10)=0.d0
      ys(11)=0.d0
      ys(12)=0.d0
      ys(13)=0.d0
      ys(14)=0.d0
      ys(15)=1.d0

      if (isfw-5) 34,34,200
200   write(*,201) xs,ys(1),ys(2),ys(3),ys(4),ys(5)
      write(1,201) xs,ys(1),ys(2),ys(3),ys(4),ys(5)
201   format(1x,f6.3, 5(d14.6))

34    isr=0
      inf=1

3     call rnktgl(n,isr,xs,dx,ndxw,ys,xfc,y,q)

      if (isfw-5) 45,45,300
300   write(*,201) xfc,y(1),y(2),y(3),y(4),y(5)
      write(1,201) xfc,y(1),y(2),y(3),y(4),y(5)

45    if(inf-ndnf) 4,5,5
4     inf=inf+1
      isr=isr+1
      go to 3

5     a1= y(7)**2 + y(9)**2 + y(8)**2 + y(10)**2
      b1= y(7)*y(12)+y(9)*y(14)+y(8)*y(13)+y(10)*y(15)
      c1= -(y(2)*y(7)+y(4)*y(9)+y(3)*y(8)+y(5)*y(10))
      a2= b1
      b2= y(12)**2 + y(14)**2 + y(13)**2 + y(15)**2
      c2= -(y(2)*y(12)+y(4)*y(14)+y(3)*y(13)+y(5)*y(15))

      det= a1*b2 - b1*a2
      dz= (c1*b2 - b1*c2)/det
      dw= (a1*c2 - c1*b1)/det
      e = y(2)**2 + y(3)**2 + y(4)**2 + y(5)**2
      z = z+dz
      w = w+dw

      if (dabs(dz/z) .gt. dzmax .or. dabs(dw/w)
     +     .gt. dwmax) go to 1
      if ( e-emax) 13,14,14

14    ndnf=ndnf+nf
```

```
        go to 1
13      if (isfw-5) 401,401,402
401     isfw=isfw+10
        z=z-dz
        w=w-dw
        go to 1

402     write(*,203) e
        write(1,203) e
203     format(3x,'e=',d16.8)
800     continue
        stop
        end


*.....................................................


        subroutine rnktgl (n,isr,xs,dx,ndxw,ys,xfc,y,q)

        implicit real*8(a-h,o-z), integer(i-n)
        dimension ys(50), f(50), y(50), q(50)
        common/paramt/pn,rn,gw,pr


        a1=0.5d+00
        a2=0.1d+01-dsqrt(0.5d+00)
        a3=0.1d+01+dsqrt(0.5d+00)
        a4=0.1d+01/0.6d+01

        if(isr) 1,1,3
1       x=xs
        do 2 i=1,n
         y(i)=ys(i)
         q(i)=0.d0
2       continue

3       idx=1

5       call fnlist(x,y,f)

        do 10 i=1,n
         dk1=dx*f(i)
         y(i)=y(i) + a1*(dk1-0.2d+01*q(i))
         q(i)=q(i) + 0.3d+01*a1*(dk1-0.2d+01*q(i))-a1*dk1
10      continue

        x=x + 0.5d+00*dx
```

```
        call fnlist(x,y,f)

        do 20 i=1,n
         dk2=dx*f(i)
         y(i)=y(i) + a2*(dk2-q(i))
         q(i)=q(i) + 0.3d+01*a2*(dk2-q(i)) - a2*dk2
20      continue

        call fnlist(x,y,f)

        do 30 i=1,n
         dk3=dx*f(i)
         y(i)=y(i) + a3*(dk3-q(I))
         q(i)=q(i) + 0.3d+01*a3*(dk3-q(i)) - a3*dk3
30      continue

        x=x + 0.5d+00*dx

        call fnlist(x,y,f)

        do 40 i=1,n
         dk4=dx*f(i)
         y(i)=y(i) + a4*(dk4-0.2d+01*q(i))
         q(i)=q(i) + 0.3d+01*a4*(dk4-0.2d+01*q(i))-a4*dk4
40      continue

        if (idx-ndxw) 41,42,42
41      idx=idx+1
        go to 5
42      xfc=x

        return
        end


*.....................................................


        subroutine fnlist(x,y,f)

        implicit real*8(a-h,o-z), integer(i-n)
        dimension y(50), f(50)
        common/paramt/pn,rn,gw,pr


        rnn=1.d0 + rn
        sum1=1.d0-pn
        sum2=2.d0-pn
        sum3=sum1/2.d0
        pi=3.141592d+00
```

```
      f(1)=y(2)
      f(2)=y(3)
      if (y(3) .gt. 0.0d+00) go to 100
      if (y(3) .lt. 0.0d+00) go to 200
      if (y(3) .eq. 0.0d+00) go to 300
100   f(3)=-((pn+1)*y(3)/2.d0+x**(sum3)*4.d0**(sum1)*
     +       (y(1)*y(3)**(sum2)/2.d0-y(2)**2*y(3)**
     +       (sum1)/6.d0+y(4)*y(3)**(sum1)/8.d0))/(pn*x)
      go to 400
200   yy1=(cos(sum1*3.141592d+00))*(-y(3))**sum1
      yy2=(cos(sum2*3.141592d+00))*(-y(3))**sum2
      f(3)=-((pn+1)*y(3)/2.d0 + x**(sum3)*4.d0**(sum1)*
     +       (y(1)*yy2/2.d0-y(2)**2*yy1/6.d0+y(4)*yy1/
     +        8.d0))/(pn*x)
      go to 400
300   f(3)=0.0d+00
      go to 400
400   f(4)=y(5)
      f(5)=-(y(5)+(pr/6.d0)*(y(2)*y(4)+3.d0*y(1)*y(5)))/x
      f(6)=y(7)
      f(7)=y(8)
      if (y(3) .gt. 0.0d+00) go to 500
      if (y(3) .lt. 0.0d+00) go to 600
      if (y(3) .eq. 0.0d+00) go to 700
500   f(8)=-((pn+1)*y(8)/2.d0+x**(sum3)*4.d0**(sum1)*
     +       ((y(6)*y(3)**(sum2)+(sum2)*y(1)*y(3)**
     +       (sum1)*y(8))/2.d0-((sum1)*y(3)**(-pn)*
     +       y(8)*y(2)**2+2.d0*y(3)**(sum1)*y(2)*y(7))
     +       /6.d0+(y(9)*y(3)**(sum1)+(sum1)*y(3)**
     +       (-pn)*y(8)*y(4))/8.d0))/(pn*x)
      go to 800
600   ss1=(cos(sum1*3.141592d+00))*(-y(3))**sum1
      ss2=(cos(sum2*3.141592d+00))*(-y(3))**sum2
      ss3=(cos(-pn*3.141592d+00))*(-y(3))**(-pn)
      f(8)=-((pn+1)*y(8)/2.d0+x**(sum3)*4.d0**(sum1)*
     +       ((y(6)*ss2 + (sum2)*y(1)*ss1*y(8))/2.d0-
     +       ((sum1)*ss3*y(8)*y(2)**2 + 2.d0*ss1*y(2)*
     +       y(7))/6.d0+(y(9)*ss1+(sum1)*ss3*y(8)*y(4))
     +       /8.d0))/(pn*x)
      go to 800
700   f(8)=-((pn+1)*y(8)/2.d0)/(pn*x)
      go to 800
800   f(9)=y(10)
      f(10)=-(y(10)+(pr/6.d0)*(y(7)*y(4)+y(2)*y(9)+3.d0*
     +        y(6)*y(5) + 3.d0*y(1)*y(10)))/x
      f(11)=y(12)
      f(12)=y(13)
      if (y(3) .gt. 0.0d+00) go to 900
      if (y(3) .lt. 0.0d+00) go to 1000
      if (y(3) .eq. 0.0d+00) go to 1100
```

```
900     f(13)=-((pn+1)*y(13)/2.d0 + x**(sum3)*4.d0**(sum1)*
     +          ((y(11)*y(3)**(sum2)+(sum2)*y(1)*y(3)**
     +          (sum1)*y(13))/2.d0 - ((sum1)*y(3)**(-pn)*
     +          y(13)*y(2)**2+2.d0*y(3)**(sum1)*y(2)*y(12))/
     +          6.d0+(y(14)*y(3)**(sum1)+(sum1)*y(3)**(-pn)*
     +          y(13)*y(4))/8.d0))/(pn*x)
        go to 1200
1000    vv1=(cos(sum1*3.141592d+00))*(-y(3))**sum1
        vv2=(cos(sum2*3.141592d+00))*(-y(3))**sum2
        vv3=(cos(-pn*3.141592d+00))*(-y(3))**(-pn)
        f(13)=-((pn+1)*y(13)/2.d0+x**(sum3)*4.d0**(sum1)*
     +          ((y(11)*vv2 + (sum2)*y(1)*vv1*y(13))/2.d0-
     +          ((sum1)*vv3*y(13)*y(2)**2 + 2.d0*vv1*y(2)*
     +           y(12))/6.d0+(y(14)*vv1 + (sum1)*vv3*y(13)*
     +           y(4))/8.d0))/(pn*x)
        go to 1200
1100    f(13)=-((pn+1)*y(13)/2.d0)/(pn*x)
        go to 1200
1200    f(14)=y(15)
        f(15)=-(y(15)+(pr/6.d0)*(y(12)*y(4)+y(2)*y(14)+
     +           3.d0*y(11)*y(5) + 3.d0*y(1)*y(15)))/x


        return
        end
```

VITA

Woo-kum Lee was born in Seoul, Korea on November 18, 1959. He attended elementary school in that city. He graduated from Seoul High School in February 1978. In March 1978 he entered Sung Kyun Kwan University in Seoul, Korea, and received a Bachelor of Science degree in Mechanical engineering in February 1982. In March of 1982, he joined the Korean Army as an ordnance officer. Upon his discharge from the Army in July 1984, he went to work as an engineer with the Dae Woo Motors Company in Inchon, Korea.

Shortly after working for the Dae Woo Motors Company, the author entered the Graduate School of the University of tennessee, Knoxville. He received the Master of Science degree with a major in engineering science in July 1988.